coatings

MDPI

Review

Thin-Film Sensors for Industry 4.0: Photonic, Functional, and Hybrid Photonic-Functional Approaches to Industrial Monitoring

Muhammad A. Butt

Institute of Microelectronics and Optoelectronics, Warsaw University of Technology, Koszykowa 75, 00-662 Warsaw, Poland; ali.butt@pw.edu.pl

Abstract

The transition toward Industry 4.0 requires advanced sensing platforms capable of delivering real-time, high-fidelity data under extreme industrial conditions. Thin-film sensors, leveraging both photonic and functional approaches, are emerging as key enablers of this transformation. By exploiting optical phenomena such as Fabry–Pérot interference, guided-mode resonance, plasmonics, and photonic crystal effects, thin-film photonic devices provide highly sensitive, electromagnetic interference-immune, and remotely interrogated solutions for monitoring temperature, strain, and chemical environments. Complementarily, functional thin films including oxide-based chemiresistors, nanoparticle coatings, and flexible electronic skins extend sensing capabilities to diverse industrial contexts, from hazardous gas detection to structural health monitoring. This review surveys the fundamental optical principles, material platforms, and deposition strategies that underpin thin-film sensors, emphasizing advances in nanostructured oxides, 2D materials, hybrid perovskites, and additive manufacturing methods. Application-focused sections highlight their deployment in temperature and stress monitoring, chemical leakage detection, and industrial safety. Integration into Internet of Things (IoT) networks, cyber-physical systems, and photonic integrated circuits is examined, alongside challenges related to durability, reproducibility, and packaging. Future directions point to AI-driven signal processing, flexible and printable architectures, and autonomous self-calibration. Together, these developments position thin-film sensors as foundational technologies for intelligent, resilient, and adaptive manufacturing in Industry 4.0.

Keywords: photonic sensors; chemical monitoring; thin-film sensors; Industry 4.0; flexible and wearable sensors; hybrid photonic-functional sensors; strain and stress sensing; IoT-enabled sensing

Check for updates

Academic Editor: Arūnas Ramanavičius

Received: 15 December 2025
Revised: 6 January 2026
Accepted: 8 January 2026
Published: 12 January 2026

Copyright: © 2026 by the author. Licensee MDPI, Basel, Switzerland. This article is an open access article distributed under the terms and conditions of the Creative Commons Attribution (CC BY) license.

1. Introduction

The rapid evolution of Industry 4.0 has reshaped manufacturing and process industries by introducing automation, cyber-physical systems, and real-time data-driven decision-making [1,2]. At the core of this transformation lies the ability to acquire continuous, high-fidelity information about operational parameters such as temperature, strain, stress, pressure, and chemical composition [3,4]. Industrial monitoring underpins critical activities ranging from predictive maintenance in aerospace turbines and chemical reactors to structural health monitoring of pipelines and smart factories [5,6]. However, many sensing technologies traditionally employed in these domains, which are predominantly

based on electronic transduction, can encounter practical limitations when deployed in certain next-generation manufacturing environments [7].

Electronic sensors constitute the backbone of industrial monitoring due to their maturity, cost-effectiveness, and ease of integration into conventional control systems. In many applications operating under moderate temperatures and benign electromagnetic conditions, electronic transduction provides reliable and high-performance sensing solutions. However, in specific industrial environments characterized by strong electromagnetic fields, high voltages, or limited accessibility, electromagnetic interference (EMI) can complicate signal integrity and system design [8]. In addition, long-term performance in harsh conditions such as elevated temperatures, chemically aggressive atmospheres, or mechanically demanding settings can be constrained by material degradation, interfacial stability, and packaging rather than by the electronic transduction mechanism itself [9].

In these contexts, photonic thin-film sensors offer complementary capabilities, including intrinsic immunity to electromagnetic interference (EMI), passive or remote optical interrogation, and compatibility with extreme or hazardous environments [7,10]. Rather than replacing electronic sensors, photonic and hybrid photonic–functional approaches address application domains where conventional electronic solutions face practical limitations, thereby expanding the available sensing toolkit for Industry 4.0-enabled manufacturing systems [11].

By harnessing optical phenomena such as Fabry–Pérot interference [12], surface plasmon resonance [13,14], guided-mode resonance [15,16], and photonic crystal effects [17], photonic thin films can be engineered to exhibit strong and selective responses to environmental perturbations [10,18–20]. Variations in refractive index, thickness, absorption, or scattering are translated into measurable optical signals with high sensitivity and stability, enabling reliable monitoring in distributed and hard-to-access industrial environments [21–24].

The versatility of photonic thin films arises not only from their transduction mechanisms but also from the broad palette of functional materials available. Metal oxide films such as ZnO [25], TiO_2 [25], SnO_2 [25,26], and WO_3 [27] are widely studied for their chemical reactivity and robustness, making them suitable for gas detection and environmental monitoring [28]. Noble metals (Au, Ag, Al) facilitate strong plasmonic resonances [14,29,30], enhancing sensitivity in refractometric and biosensing applications. In parallel, emerging nanomaterials, including graphene [31,32], MoS_2 [33], and hexagonal boron nitride [34], bring exceptional surface-to-volume ratios, tunable bandgaps, and strong light–matter interactions. Additionally, perovskites [35] and hybrid organic–inorganic films [36] offer unique combinations of optical nonlinearity, defect tolerance, and facile processing routes, opening new directions for multi-functional sensing. Progress in thin film deposition methods, such as atomic layer deposition (ALD), for atomic-scale control [37], chemical vapor deposition (CVD) for scalable growth [38,39], sputtering for robust coatings, and printing for low-cost flexible devices, further accelerates the adoption of these sensors across industrial sectors [20,40].

The role of thin-film photonic sensors in Industry 4.0 extends beyond isolated measurements [7,41,42]. Their integration into cyber-physical systems, Internet of Things (IoT) architectures, and digital twins enable real-time feedback loops between physical processes and virtual models. For example, thin film optical coatings on fiber networks can provide distributed sensing for temperature gradients in reactors, strain profiles in aerospace structures, or chemical leakage in pipelines, feeding data directly into predictive algorithms for early fault detection [42]. The convergence of nanophotonic design, materials science, and machine learning is expected to further enhance the interpretability and predictive

power of sensor outputs, accelerating the transition toward self-diagnosing, autonomous industrial systems [43,44].

While photonic thin-films represent a major thrust of this review, it is equally important to recognize that many thin-film sensors for Industry 4.0 operate via functional mechanisms beyond optics. These include chemiresistive metal-oxide coatings [45,46], piezoresistive nanoparticle films [47], flexible polymer-based electronic skins [48,49], and hybrid organic–inorganic composites [50]. Collectively, these functional devices complement optical platforms by addressing environments where optical interrogation is challenging or where low-cost, disposable sensing is desired. In this sense, thin-film sensors, whether photonic, functional, or hybrid, should be viewed as a continuum of technologies that together form the foundation of resilient and adaptive industrial monitoring in the era of Industry 4.0 [7,51].

In this review, the term "hybrid" is used in a broad and deliberate sense. It refers not only to hybrid material systems, such as organic–inorganic or multi-component thin films, but also to hybrid sensor architectures that integrate photonic and functional transduction mechanisms within a single platform [52,53]. Such hybrid approaches combine the strengths of optical sensing (e.g., electromagnetic interference immunity, remote interrogation, and high sensitivity) with functional responses such as chemiresistive, piezoresistive, or electrochemical transduction [54,55]. Throughout the manuscript, the term "hybrid" is used consistently to describe thin-film sensors that merge these complementary material and device-level functionalities, rather than implying a purely material-based hybridization alone.

This review aims to provide a comprehensive assessment of thin-film photonic sensors within the context of Industry 4.0, focusing on their deployment for temperature, strain, and chemical monitoring in industrial environments (Figure 1). Section 2 outlines the fundamental optical principles, material platforms, and deposition techniques relevant to photonic thin films. Section 3 surveys their application across key domains, including thermal management, structural health monitoring, and hazardous chemical detection, highlighting both laboratory demonstrations and industrial case studies. Section 4 examines strategies for industrial integration and smart manufacturing, while Section 5 discusses the challenges and limitations that remain in scaling these devices for widespread adoption. Finally, Section 6 explores future research directions, including the use of nanostructured and flexible films, AI-assisted sensing, and autonomous calibration systems. By bridging the gap between fundamental photonic thin film research and practical industrial deployment, this review underscores the transformative potential of these devices in enabling safe, efficient, and intelligent manufacturing. Rather than exhaustively reviewing every thin-film sensing technology, this review adopts an application-driven perspective, focusing on representative photonic, functional, and hybrid thin-film platforms that illustrate cross-cutting design principles, performance trade-offs, and integration challenges relevant to Industry 4.0.



Figure 1. Flowchart of the review structure on thin-film sensors for Industry 4.0. The paper discusses fundamental principles, key applications, integration aspects, major challenges, and future directions, highlighting the role of thin-film sensors in enabling intelligent and resilient industrial monitoring.

2. Fundamentals of Photonic Thin Films

In the context of Industry 4.0, functional thin films represent a broad class of engineered coatings designed to impart sensing, actuation, or transduction capabilities through optical, electrical, mechanical, or chemical responses. These films include inorganic, polymeric, hybrid, and nanostructured materials fabricated using a wide range of deposition and printing techniques. Photonic thin films constitute a specific and strategically important subclass of functional thin films, in which the sensing mechanism relies primarily on light–matter interaction, such as interference, waveguiding, plasmonic resonance, or photonic bandgap modulation. Although many materials and fabrication approaches are shared across functional thin-film technologies, photonic implementations distinguish themselves through contactless interrogation, immunity to electromagnetic interference, and compatibility with harsh industrial environments.

Accordingly, this review considers functional thin films as the general technological platform, while emphasizing photonic and hybrid photonic–functional sensors as preferential solutions for industrial monitoring. This perspective enables a unified discussion of deposition techniques while highlighting the advantages of optical transduction for distributed, robust, and scalable sensing architectures required in Industry 4.0.

Thin-film photonics is based on controlling light–matter interactions within nanostructures whose thickness typically ranges from a few nanometers to several micrometers [56]. Such films form the functional backbone of many optical sensors, where changes in optical path length, refractive index, or absorption provide a direct means of transducing temperature, strain, or chemical variations [57]. Their utility in Industry 4.0 lies in the possibility of mass manufacturing, miniaturization, and integration with electronic and photonic platforms. The operation of thin-film photonic sensors relies on well-defined optical principles, precise deposition strategies, the choice of advanced material systems, and effective approaches for integration.

2.1. Optical Principles

The sensing response of photonic thin-films is rooted in a set of fundamental optical phenomena [58]. Thin-film interference arises from the phase difference between light waves reflected and transmitted at successive interfaces, producing wavelength-dependent constructive or destructive interference. Small perturbations in film thickness or refractive index, induced by temperature fluctuations, strain, or analyte adsorption, result in measurable spectral shifts [59].

Waveguiding effects are equally critical. When a thin film of sufficiently high refractive index is bounded by lower-index layers, guided modes can be sustained through total internal reflection [60]. The effective index of these modes is strongly influenced by environmental changes, as the evanescent field extends into the surrounding medium. This property makes waveguide-based thin-film sensors highly responsive to local refractive index modifications or surface adsorption events. Zhou et al. introduced a compact, portable planar waveguide-based evanescent wave immunosensor (EWI) designed for the ultrasensitive detection of bisphenol A (BPA)as shown in Figure 2a [61]. Light was coupled into the planar waveguide chip through a beveled facet, where total internal reflection generates an evanescent field that excites fluorophore-labeled antibodies immobilized on the chip surface (Figure 2b). The sensor achieved a detection limit as low as 0.03 μg/L for BPA, with a linear response spanning 0.124–9.60 μg/L and a 50% inhibition concentration of 1.09 ± 0.25 μg/L. The planar waveguide chip demonstrated strong reusability, sustaining more than 300 assay cycles with each measurement completed in ~20 min. Following an optimized sample pretreatment protocol, recovery tests in real water samples yielded values between 88.3% ± 8.5% and 103.7% ± 3.5%, confirming the device's suitability for practical BPA monitoring [61].

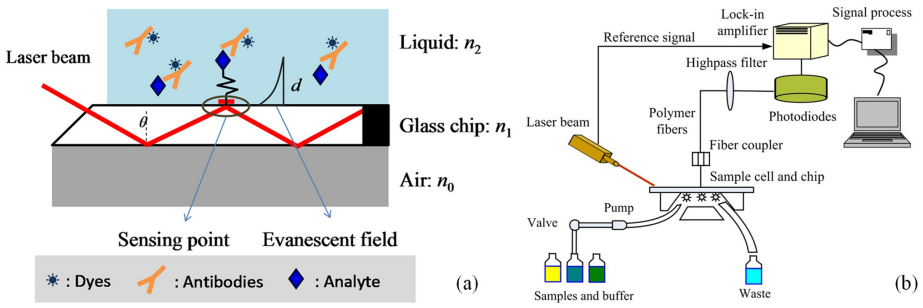


Figure 2. (**a**) Conceptual illustration of the planar optical waveguide chip operating via evanescent field. (**b**) Diagram of the planar waveguide-based immunosensing setup utilizing the evanescent wave [61].

Plasmonic effects provide another powerful transduction pathway. Noble metal thin films support surface plasmon polaritons at metal–dielectric interfaces and localized resonances in nanostructured films [62]. These resonances, stemming from collective electron oscillations, exhibit sharp spectral features with extreme sensitivity to nanoscale variations in the dielectric environment. Such characteristics enable label-free detection in chemical and biosensing applications [63]. Finally, photonic crystal thin films, created by introducing periodic variations in refractive index, generate photonic bandgaps that restrict light propagation within certain frequency ranges [64]. The presence of lattice defects produces localized resonant modes whose frequencies shift in response to external perturbations, offering narrowband and high-quality-factor sensing elements [65].

2.2. Deposition Techniques

The fabrication method determines the structural, optical, and mechanical performance of thin-film sensors. Physical vapor deposition techniques such as magnetron sputtering yield dense, uniform oxide and metallic films with excellent adhesion and controllable thickness, making them reliable for high-performance sensing elements [66]. Atomic layer deposition (ALD), based on sequential self-limiting surface reactions, allows angstrom-level thickness precision and conformal coverage on complex geometries, which is indispensable for nanoscale resonators and waveguides [67,68].

Solution-based approaches such as sol–gel processing offer a low-cost route to producing oxide thin films with tunable porosity and surface area, thereby enhancing analyte inter-

action [69–71]. Chemical vapor deposition (CVD), and its plasma-enhanced variants enable the growth of high-purity crystalline thin films, particularly suited for two-dimensional materials and perovskites [37,72]. More recently, additive manufacturing strategies such as inkjet or aerosol jet printing have emerged as scalable methods for depositing patterned functional films on rigid and flexible substrates, aligning with the requirements of Industry 4.0 for customizable, large-area sensor fabrication [73–75].

The performance and reliability of thin-film photonic sensors are critically dependent on the deposition technique used to fabricate the sensing layers. Each deposition route determines the resulting film's thickness precision, surface morphology, crystallinity, porosity, and adhesion, parameters that directly influence optical resonance quality, sensitivity, and long-term stability in harsh industrial environments. Conventional methods such as sputtering and ALD enable dense, conformal coatings with precise nanoscale control, while solution-based sol–gel processing and printing techniques offer scalable, low-cost fabrication routes aligned with Industry 4.0 requirements for customization and flexibility. High-purity methods such as CVD and MBE further extend opportunities to integrate advanced 2D materials and semiconductor films into photonic architectures. To contextualize their role in thin film sensor fabrication, Table 1 compares the working principles, achievable precision, material compatibility, advantages, limitations, and industrial readiness of the major deposition techniques.

Table 1. Thin-film deposition techniques for functional thin-film elaboration in Industry 4.0.

Deposition Technique	Working Principle	Thickness Control/ Precision	Material Compatibility	Advantages	Limitations	Industrial Relevance/ Industrial Applications
Magnetron Sputtering (Physical Vapor Deposition, PVD) [76,77]	Ejection of target atoms by plasma ions, deposition onto the substrate	nm–µm range, moderate precision	Oxides (ZnO, TiO_2, SnO_2, WO_3), metals (Au, Ag, Pt)	Dense, uniform films; good adhesion; scalable to large areas; robust coatings	Equipment cost; slower deposition for thick films; requires vacuum	Industrial coatings for temperature/strain sensors; tool-integrated thin-film sensors
Atomic Layer Deposition (ALD) [78,79]	Sequential self-limiting surface reactions, cycle-by-cycle growth	Å-level (0.1–0.2 nm/ cycle)	Oxides (Al_2O_3, TiO_2, HfO_2), nitrides, hybrid nanolaminates	Ultra-precise thickness; conformal coverage on 3D/porous structures; defect control	Low throughput; expensive precursors; not yet cost-effective at large scales	Nanoscale resonators, waveguides, flexible strain sensors with humidity protection
Chemical Vapor Deposition (CVD, incl. PECVD) [80,81]	Gas-phase precursors react/decompose on heated substrate	nm–µm; tunable	2D materials (graphene, MoS_2), perovskites, high-purity oxides	High-quality crystalline films; scalable; suitable for electronics integration	Requires high T (≥500 °C); precursor hazards; uniformity issues on large substrates	Growth of graphene/MoS_2 for chemical sensing; CMOS-compatible integration
Sol–Gel Processing [69,82]	Hydrolysis/ condensation of metal alkoxides → gel → thin film via spin/dip coating	10 s–100 s of nm	SiO_2, TiO_2, ZnO, hybrid organic–inorganic	Low cost; tunable porosity; easy doping; large-area deposition	Shrinkage/ cracking during annealing; lower density vs. PVD/ALD	Porous oxide films for chemical sensing (gas/VOC detection)
Inkjet/Aerosol Jet/Screen Printing (Additive Manufacturing) [83–85]	Direct deposition of functional inks in patterned form	µm-scale thickness, patternable	Polymers, hybrid films, nanomaterials (graphene inks, oxides)	Maskless, scalable, flexible substrates (PET, PDMS); Industry 4.0 friendly	Lower resolution vs. lithography; ink formulation critical; surface roughness	Flexible/wearable photonic sensors, disposable chemical detectors
Molecular Beam Epitaxy (MBE) [86–88]	Evaporation of elemental beams under UHV; epitaxial growth	Sub-nm precision	III–V semiconductors, perovskites	High-purity, defect-free films; precise bandgap tuning	Very costly; ultra-slow; limited scalability	Prototype quantum/photonic structures, research-scale TFPS (thin film photonic sensors)

2.3. Material Platforms

The choice of materials plays a decisive role in defining the optical response, sensitivity, and environmental stability of thin-film sensors [89–91]. Accordingly, the following discussion emphasizes not only representative material platforms, but also the physical mechanisms, performance limitations, and design rules that govern their applicability in thin-film photonic sensors. Metal oxides represent one of the most established classes: zinc oxide (ZnO) combines semiconducting and piezoelectric properties, making it useful for UV and strain sensing [92]; titanium dioxide (TiO_2), with its high refractive index and chemical stability, is widely employed in interference coatings and waveguide structures [93]; tin dioxide (SnO_2) exhibits strong gas adsorption sensitivity, which underpins its role in environmental monitoring [94]; and tungsten trioxide (WO_3) demonstrates electrochromic and gasochromic responses relevant for chemical detection [95].

In addition to these widely studied oxides, perovskite-type semiconducting metal oxides such as barium strontium titanate ($BaSrTiO_3$) have attracted increasing attention for sensing applications. $BaSrTiO_3$ thin films can be readily fabricated using sol–gel techniques, enabling low-cost processing, compositional tunability, and uniform large-area coatings [96]. Owing to their mixed ionic–electronic conduction, tunable band structure, and strong surface reactivity, $BaSrTiO_3$-based thin films have demonstrated promising performance in gas-sensing applications, particularly for the detection of oxidizing and reducing gases. Recent studies have highlighted the suitability of sol–gel-derived $BaSrTiO_3$ thin films for integration into semiconducting gas sensors, further reinforcing the importance of metal oxides as versatile material platforms for thin-film sensing technologies [97].

Noble metals such as gold, silver, and aluminum are central to plasmonic thin-film platforms. Gold is chemically stable and biocompatible, serving as the material of choice for surface plasmon resonance (SPR) biosensing [98]. Silver provides the strongest plasmonic enhancement but is limited by susceptibility to oxidation, while aluminum supports plasmonic effects in the ultraviolet regime and is attractive for Complementary Metal–Oxide–Semiconductor (CMOS)-compatible integration [99,100].

In recent years, two-dimensional (2D) materials have become important components of thin-film photonics. Graphene, with its tunable optical conductivity and broadband absorption, is highly responsive to environmental perturbations and electrical gating [31]. Transition metal dichalcogenides such as molybdenum disulfide (MoS_2) provide direct bandgaps in monolayer form and strong excitonic interactions, enhancing their sensitivity to molecular adsorption. Hexagonal boron nitride (h-BN), by contrast, functions as a wide-bandgap dielectric with exceptional chemical and thermal stability, frequently used as a protective layer in van der Waals heterostructures.

Hybrid perovskites, such as methylammonium lead iodide ($MAPbI_3$) [101], further enrich the material library for thin-film photonic sensing due to their strong light–matter interaction, high absorption coefficients, long carrier diffusion lengths, and composition-tunable bandgaps. While their inherent sensitivity to environmental stimuli is advantageous, challenges related to long-term stability remain unresolved. Moving beyond material listing, recent studies have clarified the performance-limiting mechanisms and emerging design rules for perovskite-based photonic sensors. However, conventional polycrystalline perovskite thin films suffer from moisture sensitivity, ion migration, and grain-boundary defects, leading to signal drift, hysteresis, and limited long-term reproducibility. Recent advances in solution-based space-confined growth of single-crystal thin-film perovskites address many of these limitations by suppressing ion migration and trap-assisted recombination, while providing improved optical stability and repeatability [102–104]. These emerging single-crystal perovskite films therefore represent a promising subclass for ro-

bust, high-precision photonic sensing, particularly in resonance-based and integrated waveguide platforms.

2.4. Integration Approaches

To translate material functionalities into practical sensor platforms, effective integration strategies are essential. On-chip integration of thin films into resonators [105], Mach–Zehnder interferometers [106], or ring waveguides, allow compact, multiplexed sensors compatible with silicon photonics and CMOS manufacturing infrastructure [107]. Fiber-optic integration, in which thin films are deposited on fiber Bragg gratings or tapered fibers, leverages evanescent-field interactions to enable remote, distributed sensing in harsh industrial environments [108,109]. Low-temperature deposition and printing methods further allow thin films to be fabricated on polymeric substrates such as polydimethylsiloxane (PDMS) or polyethylene terephthalate (PET), yielding lightweight, flexible, and wearable photonic sensors. Hybrid integration strategies, combining plasmonic films, 2D materials, and photonic crystal architectures, are increasingly adopted to maximize sensitivity and expand the range of detectable parameters, thereby aligning with the multifunctional sensing requirements of Industry 4.0 [110–112].

3. Thin Film Photonic Sensors for Industrial Applications

The industrial applications of thin-film sensors extend well beyond purely photonic implementations. Functional films based on resistive or capacitive transduction provide direct electrical readouts of temperature, strain, or chemical adsorption events, while hybrid devices that integrate photonic resonances with electronic or electrochemical elements are increasingly explored for multi-parameter monitoring. By surveying both photonic and functional approaches, this review emphasizes that thin-film sensors are not a monolithic category but a diverse toolkit adaptable to the varied demands of smart factories, energy infrastructure, and safety-critical sectors. Their inherent miniaturization, compatibility with optical and electronic platforms, and ability to transduce environmental changes into measurable signals make them ideal for real-time monitoring in Industry 4.0 environments. This section reviews thin-film sensors by application domain, focusing on temperature, strain, chemical leakage, and safety monitoring. In this context, hybrid thin-film sensors denote platforms that integrate photonic and functional sensing mechanisms to enable multi-parameter and application-specific industrial monitoring.

3.1. Temperature Monitoring

Temperature is one of the most fundamental parameters in industrial processes, from power generation to chemical manufacturing [113,114]. Thin films with strong thermo-optic responses, such as vanadium dioxide (VO_2) and other transition metal oxides, offer highly sensitive photonic sensing capabilities. VO_2 is particularly notable due to its metal–insulator phase transition near 68 °C, which leads to abrupt changes in refractive index and optical transmission, making it suitable for dynamic thermal sensing [115,116]. Similarly, oxide thin films (e.g., SiO_2, TiO_2) can be engineered for thermo-optic phase shifts in waveguide and interferometric structures. Infrared (IR) thin film coatings provide an additional route for non-contact thermal detection, enabling optical interrogation of temperature gradients on surfaces or within components [117]. Larciprete et al. systematically investigated the infrared emission of VO_2 thin films, demonstrating their potential for dynamic control of thermal radiation [116]. Using infrared thermography in the 3.5–5.1 μm range, VO_2 (80 nm) on two contrasting heat sources, a blackbody-like and a mirror-like emitter, was studied. Near its critical temperature, VO_2 behaves as a metamaterial, enabling suppression of blackbody emission and enhancement of mirror-like emissivity within a

single layer. This tunable response highlights VO_2 thin films as promising candidates for advanced infrared technologies, including thermal emitters, sensors, active filters, and detectors [116].

Importantly, thin film photonic sensors demonstrate excellent thermal stability, making them suitable for high-temperature environments such as turbines, nuclear reactors, or industrial furnaces, where conventional electronic sensors are prone to drift or failure [118,119]. Their durability and immunity to electromagnetic interference ensure accurate monitoring in extreme industrial conditions. Chen et al. presented the application of polymer-derived ceramics (PDCs) in fabricating phosphor thin-film temperature sensors [120]. A Y_2O_3: Eu phosphor film with a metal-based multilayer architecture was produced using Direct Ink Writing (DIW), achieving reliable operation above 1000 °C with a measurement error below 2.1%. The use of transition layers beneath the phosphor mitigates thermal stress mismatch and suppresses metal-induced quenching, while the inherent adhesion of PDCs ensures strong film integrity. To address oxygen sensitivity, the sensor was encapsulated with a dense, oxygen-impermeable microcrystalline glass coating, which prevents phosphorescence quenching between 300–600 °C without reducing signal intensity. In addition, DIW enabled sensor deposition on complex geometries, such as turbine blades. These combined features make PDC-based phosphor thin-film sensors suitable for precise temperature monitoring in high-temperature, oxygen-variable environments, including aircraft engine combustion chambers [120].

Recently, a composite thin-film temperature sensor was developed using oxidized SiCN precursor with La(Ca)CrO_3 fillers, fabricated by screen printing and air annealing (Figure 3a) [121]. The device operated reliably from 200 to 1100 °C with negative temperature coefficient behavior and shows only ~3% resistance drift after 1 h at 1100 °C in air. It achieved a temperature coefficient of resistance (TCR) up to −7900 ppm/°C at 200 °C, demonstrating enhanced oxidation resistance compared to earlier SiCN-based sensors (Figure 3b). This approach can be extended to other high-temperature thin-film devices such as strain gauges and heat-flux sensors for harsh-environment monitoring [121].

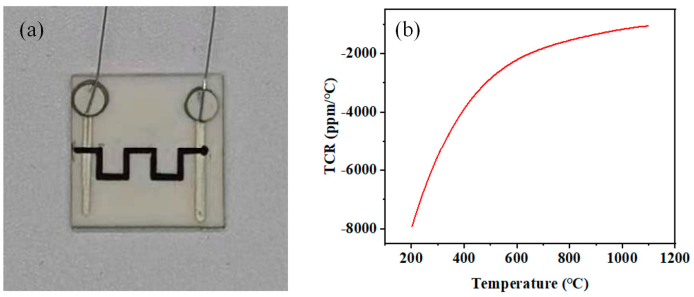


Figure 3. (**a**) LCC–SiCN composite thin-film temperature sensor following the annealing treatment, (**b**) TCR of the sensor [121].

3.2. Strain and Stress Monitoring

In modern industrial systems, continuous monitoring of mechanical stress and strain is essential for structural integrity and predictive maintenance [122]. Thin film interferometric strain sensors leverage changes in optical path length caused by deformation in the sensing layer [123,124]. By depositing thin films on substrates or integrating them with fiber-optic platforms, these sensors can detect sub-micrometer elongations and stresses [125]. Ceramic and oxide-based thin films, such as alumina or zirconia coatings, are often employed due to their mechanical robustness, thermal stability, and compatibility with harsh industrial settings. Such thin film gauges can be embedded into pipelines, aerospace structures, or mechanical components, providing real-time strain measurements for structural health monitoring (SHM) [126]. In aerospace, for instance, thin film photonic sensors enable

early detection of stress accumulation in wings or fuselage, reducing catastrophic failure risks [127]. In oil and gas pipelines, thin film coatings integrated with optical fibers detect deformation caused by pressure fluctuations or corrosion, thus preventing leaks or ruptures.

Among the various strain-sensing material platforms, platinum (Pt) nanoparticle films are discussed here as a representative case study to illustrate environmental stability and mitigation strategies, while other material systems are summarized at a class level. Aslanidis et al. investigated the performance of flexible Pt strain sensors fabricated from solvent-free nanoparticles (NPs) [122]. A new model was introduced to more accurately describe sensor response under strain, also distinguishing between solvent-free and solvent-based NP systems. Furthermore, the protective role of atomic layer deposited (ALD) Al_2O_3 coatings against humidity was examined under varying relative humidity and repeated mechanical loading. Thin films of 5 nm and 11 nm were evaluated, with the thicker coating demonstrating effective resistance stabilization even at strains up to 1.2%. The results confirm both the validity of the proposed model and the suitability of this strain-sensing approach for demanding applications such as electronic skin, flow, and pressure monitoring, while also opening pathways for computational design of NP-based devices [122].

Ultrathin electronic films can be conformally attached to the skin, enabling continuous health monitoring and real-time data visualization. Their inherent softness and mechanical flexibility minimize user discomfort, making them highly suitable for next-generation wearable technologies. For large-scale deployment, however, scalable, low-cost, and high-throughput fabrication approaches are crucial. Recent advances have demonstrated polymer light-emitting diodes (PLEDs) and organic photodetectors (OPDs) integrated into ultraflexible "optoelectronic skins" with a total thickness of only ~3 µm significantly thinner than the human epidermis [128]. By combining red and green PLEDs with OPDs, researchers developed a reflective pulse oximeter capable of monitoring blood oxygen saturation when applied to the fingertip. Furthermore, ultrathin seven-segment displays and color indicators have been utilized for direct, on-skin visualization of data [128]. As illustrated in Figure 4a, biosignals were captured by an optical sensor (Figure 4b) and subsequently displayed through either a simple color indicator (Figure 4c) or a red seven-segment digital display attached to the skin (Figure 4d). Adjusting the brightness and emission color of the PLEDs enhanced the intuitiveness and clarity of the presented information.

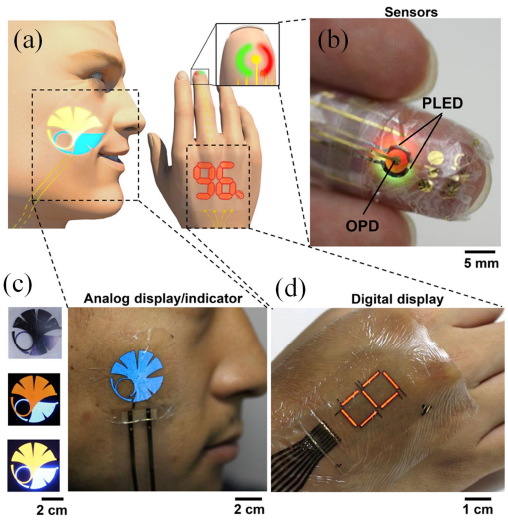


Figure 4. Example of an e-skin platform integrating health-monitoring sensors, flexible displays, and ultrathin PLEDs. (**a**) Diagram of the optoelectronic skin concept. (**b**) Image showing a fingertip with an attached organic optical sensor. (**c**) Demonstration on a human face displaying a blue and dual-color University of Tokyo logo, with brightness controlled by voltage. (**d**) Image of a red seven-segment PLED display applied on a hand [128].

At the physicochemical level, strain sensing in thin films is governed by strain-induced modulation of electronic structure and interfacial states rather than by geometric deformation alone [129]. In metallic and oxide-based films, lattice distortion modifies charge-carrier scattering, defect-state occupancy, and intergranular contact resistance, while interfaces between nanoparticles, grains, or film–substrate junctions often dominate the transduction response under mechanical loading [130]. Surface and near-surface defect states further influence strain sensitivity by regulating local charge redistribution and stress transfer efficiency, particularly in nanostructured and ultrathin films [131]. Consequently, control over defect density, film continuity, and interfacial chemistry is critical for achieving stable and repeatable strain response under cyclic and high-humidity industrial conditions.

3.3. Chemical Leakage Detection

Chemical safety is a cornerstone of Industry 4.0 operations, particularly in refineries, processing plants, and transport systems [132]. Thin-film photonic sensors play a key role in detecting chemical leaks by exploiting the optical responses of gas-sensitive films [23]. Materials such as tin oxide (SnO_2), zinc oxide (ZnO), tungsten trioxide (WO_3), and emerging 2D materials like graphene exhibit significant changes in refractive index or absorption spectra when interacting with gases like hydrogen, carbon monoxide, nitrogen oxides, or volatile organic compounds (VOCs) [133–135]. These thin films can be deposited onto waveguides, resonators, or fiber-optic probes, where gas adsorption modifies the effective refractive index, producing a measurable spectral shift. Optical fiber sensors coated with thin films are especially advantageous for leak detection in distributed networks, offering real-time, remote, and multiplexed monitoring over long distances [24,136,137]. Their passive optical nature eliminates the risk of sparks, which is critical for deployment in hazardous chemical environments. This makes thin-film photonic sensors invaluable for early-warning systems in chemical plants, storage facilities, and transportation pipelines [135].

Prasanth et al. presented the fabrication and evaluation of an evanescent-wave fiber optic VOC sensor employing a cladding modification strategy [138]. Thin films of zinc oxide (ZnO), aluminum-doped zinc oxide (AZO), and tin oxide (SnO_2) were deposited on the exposed region of an optical fiber using RF magnetron sputtering. The resulting coatings were examined through scanning electron microscopy (SEM), energy dispersive spectroscopy (EDS), X-ray diffraction (XRD), UV–Vis spectroscopy, and ellipsometry. The sensing performance of each probe was investigated for acetone, acetophenone, ethanol, and isopropanol (IPA) at concentrations between 0 and 250 ppm. Among the tested devices, the SnO_2-based probe exhibited the strongest response, reaching 21.2% for 250 ppm IPA, with response and recovery times of approximately 17 s and 21 s, respectively. Besides intensity variation, the devices also demonstrated wavelength shifts associated with lossy mode resonance. In particular, the SnO_2-coated probe achieved a maximum spectral shift of 2.4% at 250 ppm IPA and demonstrated a detection threshold down to 300 ppb [138].

Yun et al. presented a fiber-optic chemical sensor (FOCS) based on leaky-wave mode and optical time-domain reflectometry (OTDR) for detecting liquid chemical leaks [139]. Sensor nodes were fabricated by removing protective coatings through mechanical, chemical, or laser stripping, enabling dense, quasi-distributed monitoring. The system demonstrates sensitivity to liquids with varying refractive indices, supports multi-point detection, and shows potential for estimating refractive index ranges, making it suitable for leakage monitoring in diverse environments [139]. High-performance chemical sensors must detect analytes at trace levels while also distinguishing between different species. Although two-dimensional nanomaterial sensors achieve exceptional sensitivity, their selectivity remains limited. Motala et al. demonstrated a broadband fiber-optic platform coated with MoS_2 thin films, where analyte differentiation is enabled by monitoring transmission changes in

the visible spectrum under exposure to aliphatic and aromatic vapors [140]. Transmission losses align with refractive index features linked to excitonic resonances (A, B, C) and defect states. Selectivity mechanisms explored include donor–acceptor interactions, aromaticity, refractive index variations, and intercalation effects from aniline compounds. The sensor is reusable, reversible, and enables selective detection of aniline at concentrations as low as 6 ppm [140].

ZnO nanoparticle suspensions prepared through planetary ball milling (nanoinks) were employed to fabricate thin-film chemiresistive gas sensors capable of operating at room temperature [141]. By adjusting the milling parameters such as rotation speed, duration, and solvent type, thin films with controllable particle sizes and porosity were obtained and subsequently tested in dry air/oxygen environments against hydrogen, argon, and methane, as well as under varying relative humidity and ambient light. Milling speeds up to 1000 rpm yielded nanoparticles and thin-film surface roughness values below 100 nm, as confirmed through atomic force microscopy and scanning electron microscopy. Structural and compositional integrity of the ZnO was validated using Raman spectroscopy, photoluminescence, and X-ray diffraction. The optimal sensing response at room temperature was observed for suspensions processed at 400 rpm for 30 min in a mixture of ethylene glycol and deionized water, a result attributed to higher porosity and stronger modulation of electron density from oxygen ion adsorption and desorption on ZnO surfaces. Performance improved further with increased operating temperature, reaching maximum sensitivity between 100 °C and 150 °C (Figure 5a). As shown in Figure 5b, elevated temperatures also reduce response and recovery times, attributed to lower activation energy for surface reactions, enabling faster adsorption and desorption on ZnO surfaces. These results highlight the feasibility of producing low-cost, solution-processed ZnO nanoink thin films via planetary ball milling for gas and humidity sensing applications in environmental monitoring, healthcare, food packaging, laboratories, and industry [141].

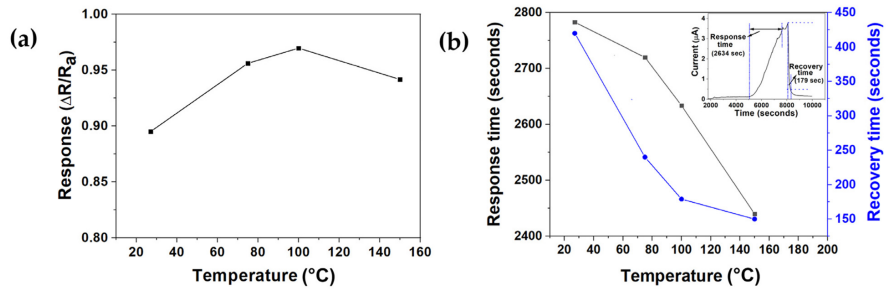


Figure 5. Influence of operating temperature on sensor performance. (**a**) Sensor response for ZnO nanoinks milled at 600 rpm for 10 min in ethylene glycol. (**b**) Response and recovery characteristics, with the inset illustrating current variation during exposure to dry air followed by argon at 100 °C [141].

3.4. Safety and Hazard Monitoring

Beyond targeted temperature, strain, or chemical sensing, thin-film photonic devices are increasingly designed to enhance overall industrial safety [142]. In fire- and explosion-prone environments, thin film coatings that respond optically to heat or combustion gases can act as early fire detectors [143,144]. Thin films functionalized for toxic chemical detection (e.g., detecting ammonia, chlorine, or sulfur-based compounds) further extend the safety portfolio of these sensors. By integrating fiber-optic networks, thin-film sensors can be distributed across large facilities, enabling comprehensive hazard mapping [145]. Their compactness allows embedding within walls, pipelines, or machine housings, creating "smart" safety layers. Importantly, thin-film photonic sensors can be integrated

with industrial alarm and automatic shutdown systems. For instance, upon detection of hazardous concentrations of toxic gases, the sensor can trigger immediate alerts or actuate process shutdown, minimizing risks to personnel and equipment [146]. This level of automation, aligned with Industry 4.0 frameworks, supports predictive and responsive safety architectures essential for next-generation industrial plants.

Ongoing industrial and technological advancements frequently lead to the emission of hazardous and toxic gases, which pose serious risks to both human health and the environment. Among various sensing materials, metal oxide nanomaterials have gained considerable attention for gas detection applications due to their high surface-to-volume ratio, excellent thermal stability, ease of synthesis, and cost-effectiveness. In particular, nickel oxide (NiO), a p-type semiconductor, has emerged as a highly promising candidate because of its superior sensitivity, good repeatability, low fabrication cost, and environmentally benign nature.

Berwal et al. synthesized NiO via a simple hydrothermal approach, and its sensing performance toward nitrogen dioxide (NO_2) was systematically investigated [147]. The structural, morphological, and optical features of the prepared NiO were examined through multiple characterization techniques, including x-ray diffraction (XRD), field emission scanning electron microscopy (FESEM), Fourier transform infrared spectroscopy (FTIR), Brunauer–Emmett–Teller (BET) analysis, and UV–Vis spectroscopy. A thin NiO film deposited on a glass substrate was tested under different concentrations of NO_2 at working temperatures ranging from 100 to 250 °C. The sensor exhibited excellent responsiveness, achieving a sensitivity of 45% toward 10 ppm of NO_2 at a relatively low operating temperature of 200 °C. Furthermore, its stable repeatability highlights its reliability, reinforcing its potential for precise and consistent NO_2 detection in practical applications [147].

Escobedo et al. developed a wearable platform for real-time CO_2 monitoring inside FFP2 masks [148]. The system combined an opto-chemical sensor with a flexible, battery-free near field communication (NFC) tag, achieving a resolution of 103 ppm, a detection limit of 140 ppm, and an operating lifetime of 8 h, consistent with the recommended usage period of FFP2 masks. A companion smartphone application enabled wireless powering, data collection, processing, alerts, and result sharing. Figure 6a shows the circuit architecture of the NFC-based sensor. The design incorporates an ultra-low-power MCU for control and data handling, an NFC dynamic tag with a custom antenna for communication and power harvesting, and a sensing module consisting of a UV LED, a digital color sensor, and a temperature sensor. As illustrated in Figure 6b, the module is positioned in front of the CO_2-sensitive membrane: the 367 nm UV LED excites the membrane, and the resulting luminescence is detected by the color sensor and processed by the MCU, with the temperature sensor providing compensation. The device operates at 4.45 mW, roughly 20% of the 22.5 mW supplied by the NFC chip, enabling battery-free functionality. Fabrication was carried out on a 125 µm PET substrate, selected for its high optical transmittance, flexibility, and thermal robustness. Images of the finished 60 × 45 mm^2 tag are provided in Figure 6c–e. Tests performed during daily activities and exercise demonstrated its utility for non-invasive health monitoring and highlighted its potential for preclinical and diagnostic applications [148].

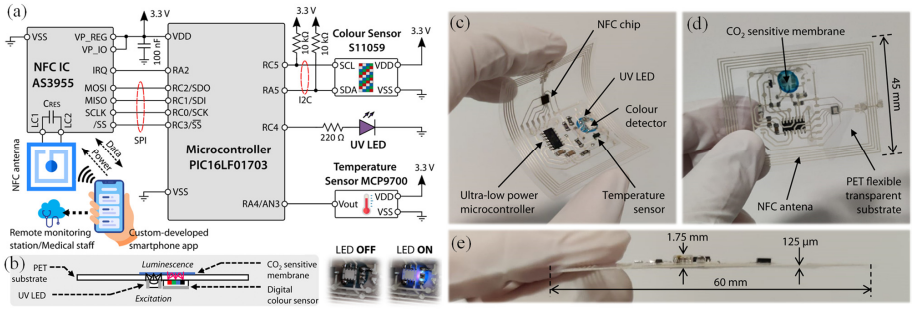


Figure 6. (**a**) Block diagram of the NFC-based circuit designed for wireless CO_2 monitoring. (**b**) Illustration of the sensing mechanism, showing the UV LED and color detector positioned opposite the CO_2-responsive membrane. The accompanying image (**right**) captures the UV excitation and red emission when the LED is activated. (**c**–**e**) Photographs of the flexible NFC tag fabricated on a 125 µm PET substrate [148].

Despite advances in cybersecurity, densely populated regions and transportation hubs remain vulnerable to improvised explosive devices (IEDs), which often contain peroxide explosives along with nitramines, nitrates, or nitroaromatics. Detecting these compounds is difficult due to their diverse chemistries and very low vapor pressures, and no existing electronic system can continuously monitor both peroxide- and nitrogen-based explosives in the vapor phase. To address this, Ricci et al. developed a thermodynamic sensor capable of ppt-level detection by measuring heat released during catalytic decomposition and redox reactions between explosive molecules and metal oxide catalysts [149]. Sensitivity and selectivity were enhanced using ultrathin, free-standing microheater films (~1 µm) fabricated through interdiffusion between a copper adhesion layer and a palladium heater element [149].

To provide a holistic overview of thin-film photonic sensors in Industry 4.0, it is essential to link specific application domains with their corresponding material platforms, optical transduction mechanisms, and industrial use cases. While Section 2 discusses deposition techniques (Table 1), the following comparison (Table 2) emphasizes how different thin-film systems are tailored to temperature, strain, chemical, and safety monitoring requirements. Where available, representative numerical ranges are included to enable rapid cross-platform comparison and decision-making. This structured summary highlights representative materials, dominant optical principles, performance benchmarks, and real-world industrial examples, enabling readers to quickly assess the suitability of each sensing approach for targeted applications.

Table 2. Application-specific comparison of thin film photonic sensors in Industry 4.0.

Application Domain	Representative Thin-Film Materials	Optical Principle Used	Key Performance Metric (Representative Values)	Industrial Example
Temperature Monitoring [116,120]	VO_2, SiO_2, TiO_2, Y_2O_3:Eu phosphor	Thermo-optic effect, phase transition, IR emission	Sensitivity: ~10–200 pm $°C^{-1}$; operating range: −50 to >500 °C; response time: <1 s to several seconds; long-term drift: <1% h^{-1}	Turbine blade monitoring, reactor temperature mapping
Strain/Stress Monitoring [125]	Pt nanoparticle films, Al_2O_3-coated sensors, ZnO	Fabry–Pérot interference, thin-film interferometry	~1–10 µε; gauge factor (hybrid/optical): ~10–10^3; dynamic range: up to several mε; fatigue endurance: >10^6 cycles	Aerospace wing/fuselage stress detection

Table 2. *Cont.*

Application Domain	Representative Thin-Film Materials	Optical Principle Used	Key Performance Metric (Representative Values)	Industrial Example
Chemical Leakage Detection [134]	SnO_2, ZnO, WO_3, MoS_2, Graphene	Refractive index change, absorption, gasochromic effect	ppb–ppm range; response/recovery time: seconds–minutes; selectivity: material-dependent; stability: hours–days without recalibration	Pipeline VOC detection, refinery gas monitoring
Safety/Hazard Monitoring [144,149]	SnO_2, SiC, hybrid oxide films	Plasmonic sensing, gasochromic, photonic crystal bandgap shift	ppb–ppm; alarm time: <10 s–minutes; operating humidity: 10%–90% RH; environmental robustness: moderate–high (platform dependent)	Fire alarms, explosive detection in transport hubs

Note: Reported values represent typical ranges extracted from the cited literature; exact performance depends on device architecture, interrogation method, analyte, and test conditions.

4. Industrial Integration and Smart Manufacturing

For thin-film sensors to move beyond laboratory demonstrations and achieve true industrial relevance, they must be integrated into the broader ecosystem of smart manufacturing. Industry 4.0 requires sensors not only to provide accurate measurements, but also to operate as interconnected nodes within cyber-physical systems, feeding data into IoT networks, enabling wireless and distributed monitoring, and supporting on-chip integration with photonic circuits. In this context, thin-film devices must bridge material-level advances with system-level demands such as scalability, connectivity, and robustness. The following subsections explore these integration pathways, highlighting their role in IoT-enabled sensing, wireless and remote operation, and seamless incorporation into photonic circuits for high-density industrial monitoring.

4.1. Role of Thin-Film Sensors in Industry 4.0 and IoT

Thin-film photonic sensors are not only measurement devices but also integral components of the cyber-physical architecture of Industry 4.0 [23]. Their ability to deliver continuous, high-fidelity data makes them well-suited for integration into Internet of Things (IoT) networks, where real-time sensor feedback drives automated decision-making [9]. These devices support predictive maintenance, adaptive process control, and digital twin implementation by linking optical signals to cloud-based or edge-computing platforms. Unlike conventional sensors that are prone to electromagnetic interference, thin-film optical platforms offer stable, interference-free communication channels, ensuring reliable data streams in electrically noisy industrial settings [150].

Liu et al. developed a portable fiber-optic surface plasmon resonance (SPR) biosensor integrated with a smartphone platform [151]. The device was mounted on a detachable phone case that holds all optical and mechanical components without obstructing the touchscreen, allowing the smartphone and sensing unit to function as a single instrument during measurements and to be separated afterward. As illustrated in Figure 7a–d, the setup includes a schematic of the system, a photograph of the sensor attached to an Android smartphone, and a 3D view of the internal opto-mechanical structure. Input and output hard-plastic cladding silica fibers (HPOF, HP 400/430-37/730E YOFC) were polished and fixed in slots on the case to align with the LED flash and the camera. A low-cost plastic lens was introduced after the optical filter to collimate the LED's red light, while black tubing minimized stray light, and fiber connectors simplified assembly and disassembly of the

sensing module. The sensing element consisted of a silica capillary stripped of its cladding and coated with a 50 nm gold layer, forming the plasmonic interface [151].

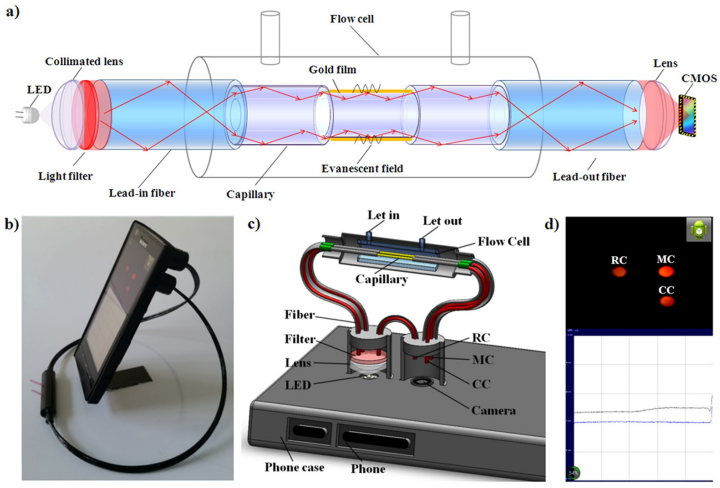


Figure 7. (**a**) Layout diagram of the smartphone-compatible SPR device. (**b**) Image of the sensor attachment mounted on an Android smartphone. (**c**) Three-dimensional illustration showing the internal design of the opto-mechanical module. (**d**) The smartphone camera acquires signals from the sensing, reference, and control channels. The captured images are analyzed in real time to extract relative intensity values, which are subsequently plotted and displayed on the phone interface [151].

Unlike conventional SPR systems with stable light sources, this design relied on the smartphone's LED flash, which was subject to intensity fluctuations. To address this, the platform incorporated three optical channels: a functionalized sensing channel for analyte detection, a non-functionalized control channel, and a reference channel to track variations in LED power. The reference fiber was positioned adjacent to the input fibers to ensure that any changes in LED intensity affected all channels equally. A dedicated smartphone application processed camera images in real time, recording channel intensities every 0.5 s to monitor refractive index changes. The biosensor's accuracy and repeatability were confirmed through antibody–antigen binding assays, with results validated against a commercial SPR instrument. This compact, cost-effective system demonstrates strong potential for portable biosensing in diagnostics, health monitoring, and environmental analysis [151].

4.2. Wireless and Remote Sensing Capabilities

A distinctive advantage of thin-film photonic sensors is their compatibility with distributed and wireless monitoring frameworks [152,153]. Fiber-optic networks coated with functional thin films can cover large industrial facilities, enabling kilometer-scale, multi-point sensing without additional wiring [154]. Remote interrogation through optical backscattering or time-domain reflectometry further reduces the need for local electronics. Emerging wireless modules (e.g., NFC, LoRa, or Bluetooth) can be coupled to photonic sensor outputs, extending their reach into portable or mobile platforms [155]. Combined with low-power optoelectronic interrogation units and energy harvesting, these systems can evolve into self-sustaining, maintenance-free sensor nodes, an essential requirement for Industry 4.0 environments [156].

Multispectral band-pass filters and a primary silver (Ag) mirror were fabricated on radiation-hardened glass substrates using ion-beam-assisted deposition for application in the optical payload of a remote sensing system [157]. The design of the filters and mirror was optimized through admittance loci analysis. Simulation results indicated that the filters could deliver average transmittance values of about 95% in the blue (B1), green (B2),

red (B3), near-infrared (B4), and panchromatic (400–900 nm) regions, while the Ag mirror exhibited an average reflectance of 99% across the visible spectrum. The deposited coatings were characterized by in situ optical monitoring, spectrophotometry, and high-resolution TEM. Experimentally, the five band-pass filters achieved average transmittance above 85% with out-of-band suppression below 1% in the 350–1100 nm range, and the protected silver mirror maintained a reflectance greater than 98%. Additional interference layers were incorporated into the protected Ag structure to further enhance reflectivity in the visible range. To assess durability for aerospace use, radiation exposure tests were conducted under simulated space conditions using a C_o^{60} gamma source with total doses up to 1 Mrad. The results confirmed that both the dielectric multilayer coatings and radiation-shielded glass substrates maintained their optical performance under these irradiation levels [157].

Furthermore, functional devices operating in the terahertz (THz) range are expected to play a critical role in advancing and deploying future 6G communication systems. A sensor was developed that combines a large active area, high responsivity, and low noise characteristics, while maintaining long-term stability at room temperature and operability under high-humidity conditions, requirements relevant to marine remote sensing and scalable manufacturing [158]. To this end, a tellurium (Te) thin film with excellent stability was fabricated, and its crystallization behavior was examined by evaluating THz sensing and detection performance after annealing at different temperatures. The optimal response was obtained after annealing at 100 °C for 60 min, yielding a sensitivity of 19.8 A/W and an equivalent noise power (NEP) of 2.8 pW Hz−1/2. The detector achieved a centimeter-scale effective sensing area, which was preserved for over two months at 30 °C in 70%–80% relative humidity without encapsulation. Owing to its robustness, large-area detection capability, and suitability for large-scale preparation, Te thin film shows strong promise as a sensor material for 6G-enabled oceanic remote sensing applications [158].

A flexible micro-3D temperature sensor based on platinum and indium oxide thermocouples was recently fabricated through microfabrication for real-time in situ monitoring [159]. Process optimization and structural design enhanced its stability, reliability, and flexibility while maintaining the rapid response of thin films. The schematic of the thin-film thermocouples (TFTCs) is shown in Figure 8a. To reduce stress from deformation, the thermoelectrode patterns were designed in a curved shape, with a 2 mm circular overlap acting as the sensing junction. Each thermoelectrode was 1 mm wide, and two rectangular pads at the terminals enabled connection for collecting the thermoelectromotive force (TEMF). Confocal laser scanning microscopy images are provided in Figure 8b,c. As seen in Figure 8b, a polyimide substrate with a wavy microstructure was fabricated to further improve resistance to deformation. The cross-section in Figure 8c shows the periodic structure with a 20 μm pitch and 2.4 μm depth. Figure 8d displays the lithographic mask under optical microscopy, while Figure 8e illustrates the resulting polyimide substrate with the designed periodic microstructure. This flexible sensor demonstrates strong potential for applications in biomedicine and robotics, including integration into face masks for health data collection and early disease detection [159].

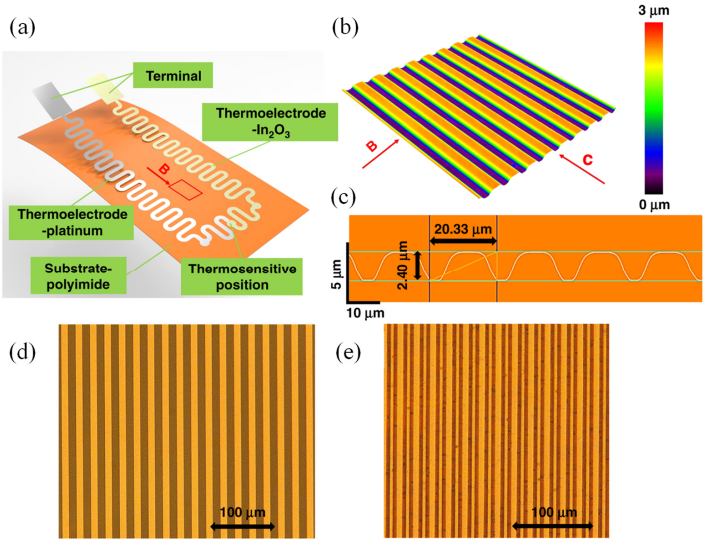


Figure 8. (**a**) Flexible micro-3D temperature sensor. (**b**) Substrate microstructure. (**c**) Cross-sectional view of the substrate. (**d**) Lithographic mask. (**e**) Polyimide substrate under optical microscopy [159].

4.3. On-Chip Integration with Photonic Circuits

For high-density industrial monitoring, thin films can be integrated directly onto photonic integrated circuits (PICs) [160–162]. This approach enables multiplexed sensing, where temperature, strain, and chemical information are captured on a single chip and processed in situ [163]. CMOS-compatible fabrication workflows allow scalable production of ring resonators, Mach–Zehnder interferometers, and plasmonic waveguides with nanoscale thin-film overlays [162,164]. Such on-chip integration reduces device footprint and simplifies packaging, while facilitating direct coupling with optoelectronic control systems. The result is compact, robust platforms capable of functioning as "smart sensing modules" embedded within industrial hardware [165].

Taharat et al. presented a CMOS-compatible plasmonic pressure sensor based on a silicon–insulator–silicon (SIS) waveguide [164]. The design integrated a rail-track resonator with grating-coupled waveguides, further enhanced by silicon nanorods in the resonator cavity. Finite element simulations showed a pressure sensitivity of 51.1 nm/MPa, exceeding reported silver-based devices and highlighting silicon's suitability for plasmonic sensing. Using silicon not only ensured compatibility with established CMOS processes but also avoided stability and tunability limitations of conventional metal sensors. The platform benefits from mature silicon photonics infrastructure and can be applied in diverse areas such as gas leakage monitoring, flow measurement, and refractive-index sensing for biomedical diagnostics, including transplant rejection detection [164].

An experimentally realized hybrid photonic–plasmonic (HPP) waveguide based on titanium nitride was reported [166]. The device employed CMOS-compatible materials and standard fabrication methods, with dielectric claddings that introduce a strong index contrast with the substrate. Compared to conventional long-range surface plasmon polariton (LRSPP) designs using noble or alternative metals, the structure achieved lower propagation loss (0.6 dB/mm) and a reduced mode size (7.7 μm). Unlike earlier approaches, it does not require index matching between substrate and cladding, enabling the use of a thin-film superstrate (~300 nm) deposited by common techniques. This design freedom supports further optimization, including epitaxial growth quality, etching selectivity, and integration with subsequent device layers. The top cladding can also be tailored, e.g., silicon nitride for photonic circuitry, active media for loss compensation, or functional oxides such as $LiNbO_3$ or ZnO for modulation without degrading performance [166].

A multifunctional, multi-channel photonic integrated chip was developed on a thin-film lithium niobate (TFLN) platform for C-band operation [167]. The compact device (1.5 cm × 0.47 cm) integrates 23 components, including multimode interference couplers, grating couplers, mode converters, phase modulators, and vertically coupled photodetectors. The chip demonstrates low channel losses (<17.5 dB), a polarization extinction ratio above 29 dB, and modulation efficiencies exceeding 4.2 V·cm across three units. These features make it a promising alternative to fiber-optic components in multi-axis optical gyroscopes, offering higher integration, reduced footprint, and lower cost.

Figure 9 presents the functional layout and working mechanism of the chip. In operation, light enters through the input port (SSC), passes sequentially through the 1 × 3 MMI coupler, two 1 × 2 MMI couplers, and the phase modulator, before exiting via the output port to the external system. Returning light is routed through the alternate port of the first 1 × 2 MMI coupler to the grating coupler, then directed to the integrated photodetector chip. The fabricated device and its functional structures are shown in Figure 9a–e [167].

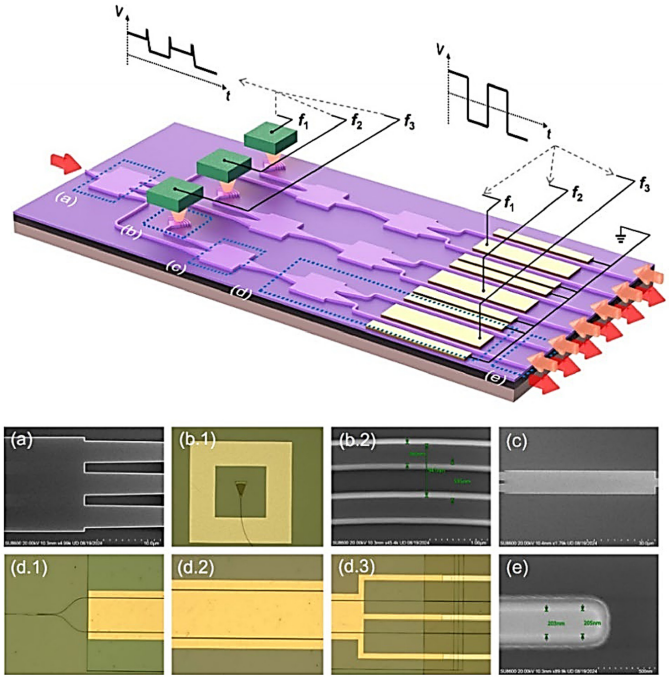


Figure 9. Structure and functionality of the TFLN multiplexing chip: (**a**) SEM image of a 1 × 3 multimode interference (MMI) coupler with three distinct output ports. (**b.1**) Wide-field optical microscope image displaying the overall configuration of the grating coupler along with a metal-assisted scattering absorption structure. (**b.2**) SEM image of the grating coupler highlighting the multilayer arc-shaped waveguide design, (**c**) SEM image of a 1 × 2 MMI coupler. (**d.1**–**d.3**) Dual-arm phase modulator layout, consisting of a 1 × 2 MMI beam splitter, a push–pull electrode arrangement, and a multilayer climbing configuration for electrode pad alignment, captured under a wide-field microscope. (**e**) SEM image of the mode spot converter, showing the tapered waveguide profile at the output end [167].

For validation, the chip was optically coupled, electrically packaged, and tested within a three-axis interferometric optical gyroscope (7200 s measurement duration, 0.1 Hz sampling rate). The system achieved bias instabilities of 0.041°/h, 0.03°/h, and 0.022°/h, and successfully measured Earth's rotation. These results demonstrate the feasibility of multifunctional TFLN photonic integrated circuits for inertial sensing and highlight their potential for miniaturizing and integrating precision measurement systems [167].

5. Challenges and Limitations

Although individual thin-film technologies differ in materials and fabrication routes, the following challenges are discussed from a cross-platform perspective, as they recur across photonic, functional, and hybrid thin-film sensors deployed in industrial environments.

5.1. Harsh Environment Durability

One of the foremost challenges facing thin-film photonic sensors in industrial applications is ensuring reliable operation in harsh environments [168,169]. Industrial facilities often expose sensing devices to corrosive gases, high humidity, abrasive particulates, or elevated temperatures [170]. Over time, these conditions can induce corrosion, mechanical fatigue, or thermal drift in thin film structures, leading to shifts in optical properties and degraded sensor accuracy [171]. For instance, long-term exposure to high-temperature cycles can alter refractive indices or cause microcracks in thin films, undermining sensor performance. Addressing these durability concerns requires protective coatings, encapsulation strategies, and the use of chemically stable materials, though such measures may increase device complexity and cost [172].

Silicon carbide (SiC), a third-generation semiconductor, has excellent mechanical, chemical, and electrical properties, which makes it well suited for pressure sensors that need to work in harsh conditions at temperatures above 300 °C. One of the main challenges, however, is the output drift that occurs at high temperatures, which reduces the accuracy and stability of the sensor. To address this, real-time temperature monitoring of the sensor chip is crucial for effective compensation. Fang et al. developed platinum (Pt) thin-film resistance temperature detectors (RTDs) on SiC substrates, introducing an aluminum oxide (Al_2O_3) transition layer to enhance adhesion and aluminum nitride (AlN) grooves for alignment during microfabrication [173]. The multilayer structure exhibited strong bonding up to 950 °C, with a stable Al_2O_3/Pt interface that ensured reliable electrical performance and good linearity above 850 °C. These properties highlight the potential of Pt RTDs for integration into SiC-based pressure sensors.

To further evaluate performance, the Pt films were annealed at different temperatures and analyzed for interfacial diffusion, surface morphology, microstructure, and electrical behavior. Figure 10a presents the schematic of the high-temperature test platform, while Figure 10b shows the laboratory-built system. The furnace temperature was calibrated between 200 and 900 °C using a K-type armored thermocouple with an accuracy of ±0.034 °C. Figure 10c illustrates the influence of annealing temperature on sheet resistance and grain size (D_{111}). Below 750 °C, sheet resistance decreased as grain size increased, consistent with reduced defects and grain boundaries. Beyond 750 °C, resistance rose sharply, reaching 1.479 Ω/sq at 950 °C—due to Pt film agglomeration and surface degradation.

The effect of annealing on the temperature coefficient of resistance (TCR) is shown in Figure 10d. Samples were annealed in air for 1.5 h at 650, 750, 850, and 950 °C, with twelve sensors tested in total. Each underwent three heating cycles from 25 to 850 °C, and representative temperature–resistance curves are shown in Figure 10e–h. The TCR reached its maximum value of 2.845×10^{-3}/°C at 650 °C, attributed to grain growth and reduced defect density. At 750 °C, pores in the film reduced TCR, while 850 °C showed partial recovery due to island thickening from agglomeration. At 950 °C, both TCR and linearity were severely degraded. Overall, the results indicate that 650 °C is the optimal annealing temperature, providing the best balance of high TCR, stability, and linearity for Pt thin-film RTDs. Preventing Pt agglomeration remains essential to further extend the operational temperature range [173].

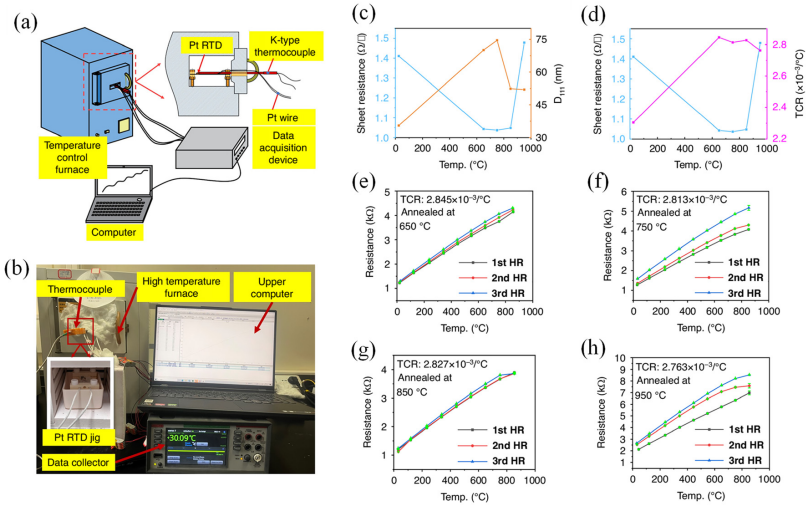


Figure 10. (**a**) Schematic of the temperature–resistance measurement setup. (**b**) Photograph of the experimental temperature–resistance platform assembled in the laboratory. (**c**) Variation in sheet resistance and Pt thin-film grain size (D111) at different annealing temperatures. (**d**) Dependence of sheet resistance and TCR on annealing temperature for Pt thin films. (**e**–**h**) Temperature–resistance curves and corresponding TCR values of Pt thin films annealed in air for 1.5 h at different temperatures [173].

5.2. Fabrication Scalability and Reproducibility

While thin film deposition and patterning technologies are well established in laboratory environments, scaling fabrication to industry-level volumes remains a significant limitation [37,56]. Many high-performance thin films rely on precise deposition methods, such as atomic layer deposition (ALD) [174] or molecular beam epitaxy (MBE) [175], which are expensive and time-intensive when applied to large-area substrates or high-throughput production. Achieving reproducibility across batches is another hurdle, as small variations in thickness, crystallinity, or surface morphology can cause large deviations in optical responses [176]. For Industry 4.0 deployment, where thousands of distributed sensors may be required, cost-effective, high-yield fabrication techniques such as roll-to-roll deposition or inkjet printing will be essential, but these are still under development for photonic-grade films [177].

5.3. Signal Stability and Cross-Sensitivity

A critical limitation of thin-film photonic sensors lies in maintaining stable and selective signals under real-world conditions. Optical responses can be influenced not only by the target analyte or parameter but also by fluctuations in temperature, humidity, or mechanical stress, leading to cross-sensitivity issues [178]. For example, a film designed for chemical vapor detection may also exhibit sensitivity to strain-induced changes in refractive index, complicating the interpretation of results. Furthermore, long-term stability is challenged by photobleaching, defect migration, or environmental contamination of the film surface [179]. Advanced signal processing, multi-parameter calibration, and the use of functionalized multilayer films are promising approaches, but these solutions introduce added complexity to sensor design [178].

5.4. Packaging and Integration with Industrial Hardware

Finally, the practical deployment of thin-film photonic sensors is often constrained by packaging and integration challenges. Industrial systems demand ruggedized sensors that can be seamlessly incorporated into existing hardware, such as pipelines, turbines, or robotic assemblies, without compromising mechanical stability or introducing significant maintenance needs. Thin films by themselves are fragile, requiring support structures or

encapsulation that can withstand mechanical vibrations and thermal cycling. Moreover, interfacing optical signals with electronic control units, industrial alarm systems, or IoT networks requires miniaturized packaging with robust fiber coupling, connectors, and protective housing. These integration steps can increase cost and reduce sensor compactness, offsetting one of the key advantages of thin film technologies. Overcoming these issues will be critical for moving from laboratory prototypes to fully functional, large-scale deployments in Industry 4.0 environments.

To systematically benchmark the current performance status, degradation mechanisms, and potential solutions of thin-film sensors in Industry 4.0, Table 3 summarizes key performance indicators (KPIs) and mitigation strategies relevant to industrial deployment.

Table 3. Technical performance benchmarks, degradation mechanisms, and mitigation strategies for thin-film sensors in Industry 4.0. The listed mitigation strategies indicate the primary mechanisms used to address the corresponding degradation modes and are representative rather than exhaustive.

Performance Metric	State-of-the-Art Values	Failure/Degradation Mechanisms	Technical Mitigation Strategies
Sensitivity/Limit of Detection (LoD) [180–182]	Gas sensors: ~100 ppb (SnO_2, MoS_2, graphene); Strain: gauge factor (GF) 5–20; Temperature: ±1–2 °C at >1000 °C	Cross-sensitivity (e.g., T–strain coupling), spectral drift, low SNR in noisy environments	Multilayer heterostructures combining plasmonic and oxide films to enhance field confinement and selectivity, bound states in the continuum resonators to increase quality factor and suppress noise, machine learning assisted spectral deconvolution to decouple overlapping temperature, strain, and chemical responses
Dynamic Range/Operating Range [183–185]	Thermal: up to 1200 °C (phosphor films, ceramics); Strain: 10^3–10^4 με; Gas conc.: 10^{-4}–10^2 ppm	Nonlinear response at high perturbations, saturation of adsorption sites, hysteresis	Adaptive calibration models to correct nonlinear behavior under large perturbations, hierarchical film architectures with nanoporous oxides and dense overlayers to delay saturation of active sites, integrated microheaters to extend operational range through controlled thermal activation
Response/Recovery Time [186–188]	Gas sensors: 10–30 s (ZnO, WO_3); Optical strain: sub-ms; Temperature: ms–s depending on film thickness	Surface reaction kinetics limited at RT, slow desorption, thermal lag in bulk substrates	Nanostructured one-dimensional and two-dimensional films to increase surface-to-volume ratio, catalytic nanoparticle doping to lower activation energy for adsorption and desorption, ultrathin conformal coatings deposited by ALD to minimize diffusion length and thermal inertia, microheater integration to accelerate recovery
Long-Term Stability/Drift [35,189,190]	Stable for months in lab; <10% drift over 10^6 cycles (strain); but severe drift under corrosive or humid atmospheres	Oxygen vacancy migration, photobleaching, film delamination, crack propagation under cyclic stress	Encapsulation using ALD Al_2O_3 or Parylene-C to suppress moisture ingress and oxygen diffusion, hydrophobic overcoats to reduce humidity-induced drift, stress-relief buffer layers to mitigate crack propagation, in situ self-calibration using reference resonators to correct long-term drift

Table 3. *Cont.*

Performance Metric	State-of-the-Art Values	Failure/Degradation Mechanisms	Technical Mitigation Strategies
Fabrication Scalability & Reproducibility [76,82,174,191]	ALD: Å-level precision, but <10 cm^2 throughput; Inkjet: 10^4 cm^2/day but µm resolution; Roll-to-roll sputtering: 10^2 m^2 scale	Batch-to-batch variability (thickness, crystallinity), ink instability, substrate-induced strain	Hybrid deposition strategies combining ALD seeding with printing to balance precision and scalability, plasma-assisted roll-to-roll sputtering to improve film uniformity, inline ellipsometry with AI-based quality control to detect deviations during fabrication
Integration/Packaging Robustness [107,160]	Fiber-integrated sensors: km-scale networks; On-chip: >20 components per PIC; Flexible e-skin: <5 µm thickness	Fiber–chip coupling loss, vibration-induced delamination, packaging thermal mismatch	CMOS-compatible integration to ensure process uniformity, ruggedized fiber arrays to reduce coupling loss, compliant encapsulation layers to absorb vibration and thermal stress, serpentine or kirigami mechanical designs to enhance flexibility and fatigue resistance
IoT/Cyber-Physical Readiness [9,192]	NFC-enabled flexible tags: power < 5 mW; Distributed fiber-optic networks with OTDR; Edge-AI latency < 10 ms	Power autonomy, cybersecurity risks, limited on-chip computing	Energy harvesting from vibration, thermal, or solar sources to enable autonomous operation, neuromorphic or edge processors to reduce latency and power consumption, physically unclonable functions and secure firmware updates to ensure data integrity

6. Emerging Trends

Accordingly, the future directions outlined here emphasize technology-agnostic trends such as AI-assisted signal processing, flexible manufacturing, and autonomous calibration that cut across multiple thin-film sensor classes rather than being specific to a single material system. One of the most transformative research directions in thin-film photonic sensors for Industry 4.0 lies in the integration of artificial intelligence (AI) and machine learning (ML) for signal processing and predictive maintenance [193–195]. The optical spectra and temporal signatures generated by thin-film structures are inherently high-dimensional, often convoluted by cross-sensitivities such as temperature–strain coupling, environmental drift, and material aging [196]. Conventional demodulation methods, which typically rely on peak tracking or polynomial fitting, lack robustness under industrial noise conditions. ML-based approaches offer a pathway to overcome these limitations by extracting latent features from spectra, classifying overlapping perturbations, and forecasting degradation pathways [197,198]. Hybrid "physics-informed" models that combine analytical transfer functions with neural-network-based residual correction have the potential to drastically reduce training data requirements while ensuring interpretability [44]. Furthermore, self-supervised and transfer learning methods can allow thin-film photonic sensors to be rapidly adapted to new materials or industrial settings, despite variations in deposition conditions or operating environments [199]. From a deployment perspective, lightweight inference architectures suitable for microcontrollers and embedded FPGAs will be critical to enable real-time, on-edge data processing with sub-10 ms latency. Beyond enhanced measurement fidelity, AI-driven predictive maintenance pipelines can model the temporal evolution of strain, corrosion, or chemical ingress, thereby supporting condition-based maintenance strategies that are aligned with the broader objectives of Industry 4.0 [200,201].

At the material and structural level, nanostructured thin films and heterostructures are poised to unlock new regimes of sensitivity and selectivity. Sensitivity in photonic sensors is governed by the overlap between the evanescent optical field and the analyte, as well as by the sharpness of the resonance condition [202]. Nanophotonic design incorporating guided-mode resonances, photonic crystals, or bound states in the continuum (BICs) can dramatically increase the quality factor (Q-factor), producing measurable spectral shifts at ppm-level changes in refractive index. Plasmonic–dielectric hybrid structures offer a complementary pathway, exploiting intense near-field enhancements while maintaining the thermal stability of dielectric films. The integration of emerging 2D materials such as graphene, transition metal dichalcogenides (TMDs), and MXenes introduces new transduction mechanisms through surface functionalization and strong optoelectronic coupling, particularly advantageous for chemical and strain sensing. Similarly, layered heterostructures combining inorganic oxides with metal–organic or covalent–organic frameworks can yield analyte-specific selectivity while maintaining compatibility with thin-film deposition workflows. Control over porosity and anisotropy, achieved via glancing-angle deposition (GLAD) [203] or block-copolymer templating [204], provides additional degrees of freedom for enhancing analyte infiltration and polarization-resolved sensing. The challenge remains in scaling these architectures through roll-to-roll sputtering [191], atomic layer deposition (ALD) [37], or nanoimprint lithography [205] while ensuring long-term stability under industrial stressors such as humidity, thermal cycling, and corrosive media.

A parallel frontier is the development of flexible and printable thin films that can be deployed rapidly on diverse industrial assets [206]. The rigid architecture typically used in photonic sensors constrains their integration on curved, dynamic, or inaccessible surfaces such as rotating machinery, robotic end-effectors, or large-diameter pipelines. Polymer-based substrates (e.g., polyimide, PEN) combined with low-loss hybrid organic–inorganic films or nanolaminate dielectrics enable mechanically robust yet optically functional platforms for conformal sensing [20]. Emerging additive manufacturing approaches, including inkjet, aerosol jet, and screen printing, facilitate the direct deposition of photonic crystals, Bragg mirrors, and plasmonic layers onto flexible substrates at scale, offering a low-cost path to disposable or temporary sensors [207]. Mechanical strategies such as kirigami and serpentine geometries mitigate strain concentration and allow operation under repeated bending cycles without compromising resonance quality [208,209]. Importantly, integration with on-foil optoelectronics such as micro-LED arrays or organic photodiodes can yield self-contained reflection-mode sensors, with wireless data transfer via near-field communication (NFC) or low-power Bluetooth [192,210]. Protective overcoats based on Parylene, ALD alumina, or fluoropolymers will be essential to ensure chemical compatibility and abrasion resistance [211]. Standardized testing protocols assessing bend fatigue, adhesion, and thermal cycling will be critical to transition these flexible sensors from laboratory demonstrations to field-ready solutions.

Looking further ahead, the ultimate vision is the realization of fully autonomous, self-calibrating thin-film photonic sensors capable of long-term, unattended operation in industrial environments [212,213]. Such autonomy requires a multi-layered strategy combining materials engineering, device design, and embedded intelligence [214]. On-chip reference resonators or etalons can provide internal calibration baselines to be correct for instrument drift, while integrated micro-heaters or electro-optic tuning elements can impose controlled perturbations for in situ calibration without interrupting process monitoring [215,216]. The concept of a “digital twin” for each sensor is an evolving computational model that incorporates film stack parameters, environmental history, and degradation kinetics can allow continuous recalibration and adaptive parameter estimation using Bayesian inference or Kalman filtering [217,218]. Autonomous energy management through vibration, thermal,

or solar energy harvesting, combined with ultra-low-power optoelectronic interrogation (<100 μW average), will reduce dependence on wired infrastructure [219]. Self-cleaning surfaces, enabled by photocatalytic coatings or antifouling fluoropolymers, will extend sensor lifetime in chemically aggressive or biofouling-prone environments [220]. Finally, robust cybersecurity and trust frameworks, leveraging physically unclonable functions (PUFs) and secure over-the-air update protocols, will be necessary to safeguard data integrity in connected Industry 4.0 networks.

Looking forward, the convergence of photonic and functional thin-film sensors is expected to yield hybrid platforms capable of unprecedented performance. For instance, devices that combine plasmonic thin films with oxide chemiresistors may leverage optical selectivity and electronic amplification simultaneously [62]. Similarly, integration of flexible piezoresistive films with optical strain gauges could enable multi-scale structural health monitoring, from local crack initiation to distributed deformation mapping [221]. Such hybridization directly aligns with Industry 4.0 objectives by creating interoperable sensing platforms that unite optical and electronic capabilities.

In summary, the future of thin-film sensors for Industry 4.0 is contingent upon simultaneous advances in intelligent signal processing, nanostructured materials, flexible manufacturing, and autonomous operation. The co-design of optical architectures with data-driven models and scalable fabrication methods will determine whether TFPS can evolve from laboratory prototypes into robust, industrial-grade platforms. Achieving this transformation will require a systematic approach to benchmarking, with key performance indicators such as long-term drift, calibration intervals, response time, and limit of detection reported alongside sensitivity. If successful, the next generation of TFPS could enable dense, reliable, and low-maintenance sensor networks that form the nervous system of Industry 4.0 manufacturing environments.

7. Summary and Outlook

Thin-film sensors are rapidly emerging as pivotal components for Industry 4.0, where continuous, high-fidelity monitoring of temperature, strain, and chemical parameters is indispensable for safe and efficient industrial operations. By combining photonic principles such as interference, plasmonics, waveguiding, and photonic crystals with functional material responses, thin films provide versatile sensing platforms that extend beyond the limitations of conventional electronic devices. Recent advances in deposition methods, ranging from atomic layer deposition and chemical vapor deposition to additive manufacturing and printing, have enabled scalable fabrication and integration on diverse substrates, including flexible and wearable platforms.

Despite this progress, several challenges remain before thin-film sensors can achieve widespread industrial adoption. Issues of durability under corrosive or thermally dynamic conditions, reproducibility across large-scale fabrication, and long-term signal stability require further attention. Packaging and seamless integration with industrial hardware and IoT networks also remain bottlenecks. Addressing these challenges will demand interdisciplinary efforts, combining materials engineering, nanophotonics, device physics, and systems-level integration. Looking ahead, emerging directions such as AI-assisted signal interpretation, flexible and conformal thin films, and autonomous self-calibrating architectures hold strong potential to transform thin-film sensors into intelligent, low-maintenance nodes within digital manufacturing ecosystems.

By presenting both photonic and functional perspectives, this review underscores that thin-film sensors should not be narrowly defined. Their value in Industry 4.0 stems from their diversity: photonic devices excel in extreme or EMI-rich environments, functional films provide low-cost and flexible solutions, and hybrid systems promise intelli-

gent, multi-modal sensing. Together, these approaches will enable dense, reliable, and scalable sensor networks that place thin-film technologies at the core of next-generation industrial monitoring.

Funding: This research received no external funding.

Institutional Review Board Statement: Not applicable.

Informed Consent Statement: Not applicable.

Data Availability Statement: No new data were created.

Acknowledgments: The author acknowledges the constant support of Warsaw University of Technology in the completion of this work.

Conflicts of Interest: The authors declare no conflicts of interest.

References

1. Folgado, F.J.; Calderón, D.; González, I.; Calderón, A.J. Review of Industry 4.0 from the Perspective of Automation and Supervision Systems: Definitions, Architectures and Recent Trends. *Electronics* **2024**, *13*, 782. [CrossRef]
2. Vaidya, S.; Ambad, P.; Bhosle, S. Industry 4.0—A Glimpse. *Procedia Manuf.* **2018**, *20*, 233–238. [CrossRef]
3. Mitrašinović, A.; Đurđević, T.; Nešković, J.; Radosavljević, M. Temperature Monitoring in Metal Additive Manufacturing in the Era of Industry 4.0. *Technologies* **2025**, *13*, 317. [CrossRef]
4. Soori, M.; Arezoo, B.; Dastres, R. Internet of Things for Smart Factories in Industry 4.0, a Review. *Internet Things Cyber-Phys. Syst.* **2023**, *3*, 192–204. [CrossRef]
5. Liehr, S. Polymer Optical Fiber Sensors in Structural Health Monitoring. In *New Developments in Sensing Technology for Structural Health Monitoring*; Mukhopadhyay, S.C., Ed.; Springer: Berlin/Heidelberg, Germany, 2011; pp. 297–333, ISBN 978-3-642-21099-0.
6. Golovastikov, N.V.; Kazanskiy, N.L.; Khonina, S.N. Optical Fiber-Based Structural Health Monitoring: Advancements, Applications, and Integration with Artificial Intelligence for Civil and Urban Infrastructure. *Photonics* **2025**, *12*, 615. [CrossRef]
7. Kalsoom, T.; Ramzan, N.; Ahmed, S.; Ur-Rehman, M. Advances in Sensor Technologies in the Era of Smart Factory and Industry 4.0. *Sensors* **2020**, *20*, 6783. [CrossRef]
8. Javaid, M.; Haleem, A.; Singh, R.P.; Rab, S.; Suman, R. Significance of Sensors for Industry 4.0: Roles, Capabilities, and Applications. *Sens. Int.* **2021**, *2*, 100110. [CrossRef]
9. Abdulhussain, S.H.; Mahmmod, B.M.; Alwhelat, A.; Shehada, D.; Shihab, Z.I.; Mohammed, H.J.; Abdulameer, T.H.; Alsabah, M.; Fadel, M.H.; Ali, S.K.; et al. A Comprehensive Review of Sensor Technologies in IoT: Technical Aspects, Challenges, and Future Directions. *Computers* **2025**, *14*, 342. [CrossRef]
10. Schott, A.; Rekowski, M.; Timmann, F.; Herrmann, C.; Dröder, K. Development of Thin-Film Sensors for In-Process Measurement during Injection Molding. *Procedia CIRP* **2023**, *120*, 619–624. [CrossRef]
11. Muthumalai, K.; Gokila, N.; Haldorai, Y.; Rajendra Kumar, R.T. Advanced Wearable Sensing Technologies for Sustainable Precision Agriculture—A Review on Chemical Sensors. *Adv. Sens. Res.* **2024**, *3*, 2300107. [CrossRef]
12. Tian, T.; Liang, K.; Ma, Y.; Geng, T. A Fabry-Perot Interferometer Based on Probe-Embedded Bubble for Ultrasensitive Strain Measurement. *Measurement* **2025**, *239*, 115505. [CrossRef]
13. Das, S.; Singh, S.; Chawla, V.; Chawla, P.A.; Bhatia, R. Surface Plasmon Resonance as a Fascinating Approach in Target-Based Drug Discovery and Development. *TrAC Trends Anal. Chem.* **2024**, *171*, 117501. [CrossRef]
14. Ahn, H.; Song, H.; Choi, J.; Kim, K. A Localized Surface Plasmon Resonance Sensor Using Double-Metal-Complex Nanostructures and a Review of Recent Approaches. *Sensors* **2018**, *18*, 98. [CrossRef]
15. Rehman, A.U.; Khan, Y.; Irfan, M.; Choudri, S.; Khonina, S.N.; Kazanskiy, N.L.; Butt, M.A. Three-Dimensional Modeling of the Optical Switch Based on Guided-Mode Resonances in Photonic Crystals. *Micromachines* **2023**, *14*, 1116. [CrossRef]
16. Fallah, H.; Hakim, L.; Boonruang, S.; Mohammed, W.S.; Hsu, S.H. Polymer-Based Guided-Mode Resonance Sensors: From Optical Theories to Sensing Applications. *ACS Appl. Polym. Mater.* **2023**, *5*, 9700–9713. [CrossRef]
17. Li, T.; Liu, G.; Kong, H.; Yang, G.; Wei, G.; Zhou, X. Recent Advances in Photonic Crystal-Based Sensors. *Coord. Chem. Rev.* **2023**, *475*, 214909. [CrossRef]
18. Butt, M.A. Butt Thin-Film Coating Methods: A Successful Marriage of High-Quality and Cost-Effectiveness—A Brief Exploration. *Coatings* **2022**, *12*, 1115.
19. Vitoria, I.; Gallego, E.E.; Melendi-Espina, S.; Hernaez, M.; Ruiz Zamarreño, C.; Matías, I.R. Gas Sensor Based on Lossy Mode Resonances by Means of Thin Graphene Oxide Films Fabricated onto Planar Coverslips. *Sensors* **2023**, *23*, 1459. [CrossRef] [PubMed]

20. Butt, M.A. Photonics on a Budget: Low-Cost Polymer Sensors for a Smarter World. *Micromachines* **2025**, *16*, 813. [CrossRef] [PubMed]
21. Butt, M.A.; Kazanskiy, N.L.; Khonina, S.N.; Voronkov, G.S.; Grakhova, E.P.; Kutluyarov, R.V. A Review on Photonic Sensing Technologies: Status and Outlook. *Biosensors* **2023**, *13*, 568. [CrossRef]
22. Abedin, S.; Biondi, A.M.; Wu, R.; Cao, L.; Wang, X. Structural Health Monitoring Using a New Type of Distributed Fiber Optic Smart Textiles in Combination with Optical Frequency Domain Reflectometry (OFDR): Taking a Pedestrian Bridge as Case Study. *Sensors* **2023**, *23*, 1591. [CrossRef]
23. Butt, M.A.; Mateos, X.; Piramidowicz, R. Photonics Sensors: A Perspective on Current Advancements, Emerging Challenges, and Potential Solutions (Invited). *Phys. Lett. A* **2024**, *516*, 129633. [CrossRef]
24. Chen, B.; Zhu, Z.; Su, Z.; Yao, W.; Zheng, S.; Wang, P. Optical Fiber Sensors in Infrastructure Monitoring: A Comprehensive Review. *Intell. Transp. Infrastruct.* **2023**, *2*, liad018. [CrossRef]
25. Neogi, S.; Ghosh, R. Metal-Oxide Gas Sensors (SnO_2, Fe_2O_3, TiO_2, CoO, ZnO, NiO, CuO, and Perovskite Oxides). In *Electric and Electronic Applications of Metal Oxides*; Moharana, S., Sahu, B.B., Satpathy, S.K., Nguyen, T.A., Eds.; Metal Oxides; Elsevier: Amsterdam, The Netherlands, 2025; pp. 333–348, ISBN 978-0-443-26554-9.
26. Masuda, Y. Recent Advances in SnO2 Nanostructure Based Gas Sensors. *Sens. Actuators B Chem.* **2022**, *364*, 131876. [CrossRef]
27. Dong, C.; Zhao, R.; Yao, L.; Ran, Y.; Zhang, X.; Wang, Y. A Review on WO_3 Based Gas Sensors: Morphology Control and Enhanced Sensing Properties. *J. Alloys Compd.* **2020**, *820*, 153194. [CrossRef]
28. Arafat, M.M.; Dinan, B.; Akbar, S.A.; Haseeb, A.S.M.A. Gas Sensors Based on One Dimensional Nanostructured Metal-Oxides: A Review. *Sensors* **2012**, *12*, 7207–7258. [CrossRef]
29. Aziz, A. A Novel Plasmonic Waveguide for Extraordinary Field Enhancement of Spoof Surface Plasmon Polaritons with Low-Loss Feature. *Results Opt.* **2021**, *5*, 100116. [CrossRef]
30. Aldewachi, H.; Chalati, T.; Woodroofe, M.N.; Bricklebank, N.; Sharrack, B.; Gardiner, P. Gold Nanoparticle-Based Colorimetric Biosensors. *Nanoscale* **2017**, *10*, 18–33. [CrossRef]
31. Bai, Y.; Xu, T.; Zhang, X. Graphene-Based Biosensors for Detection of Biomarkers. *Micromachines* **2020**, *11*, 60. [CrossRef] [PubMed]
32. Butt, M.A. Graphene in Photonic Sensing: From Fundamentals to Cutting-Edge Applications. *Fundam. Res.* **2025**. [CrossRef]
33. Tagbo, P.C.; Mohamed, M.M.; Ayad, M.M.; El-Moniem, A.A. Fabrication of Flexible MoS2 Sensors for High-Performance Detection of Ethanol Vapor at Room Temperature. *Sens. Actuators Phys.* **2025**, *389*, 116531. [CrossRef]
34. Kim, S.; Fröch, J.E.; Christian, J.; Straw, M.; Bishop, J.; Totonjian, D.; Watanabe, K.; Taniguchi, T.; Toth, M.; Aharonovich, I. Photonic Crystal Cavities from Hexagonal Boron Nitride. *Nat. Commun.* **2018**, *9*, 2623. [CrossRef] [PubMed]
35. Bystrický, R.; Tiwari, S.K.; Hutár, P.; Sýkora, M. Thermal Stability of Chalcogenide Perovskites. *Inorg. Chem.* **2024**, *63*, 12826–12838. [CrossRef] [PubMed]
36. Zhang, X.; Xue, C.; Zhang, W.; Yu, L.; Wang, Q.; Que, W.; Wang, Y.; Hu, F. Multifunctional TiO_2/Ormosils Organic-Inorganic Hybrid Films Derived by a Sol-Gel Process for Photonics and UV Nanoimprint Applications. *Opt. Mater. Express* **2019**, *9*, 304–314. [CrossRef]
37. Crowell, J.E. Chemical Methods of Thin Film Deposition: Chemical Vapor Deposition, Atomic Layer Deposition, and Related Technologies. *J. Vac. Sci. Technol. A* **2003**, *21*, S88–S95. [CrossRef]
38. Nam, J.; Yang, J.; Zhao, Y.; Kim, K.S. Chemical Vapor Deposition of Graphene and Its Characterizations and Applications. *Curr. Appl. Phys.* **2024**, *61*, 55–70. [CrossRef]
39. Beliaev, L.Y.; Shkondin, E.; Lavrinenko, A.V.; Takayama, O. Optical, Structural and Composition Properties of Silicon Nitride Films Deposited by Reactive Radio-Frequency Sputtering, Low Pressure and Plasma-Enhanced Chemical Vapor Deposition. *Thin Solid Films* **2022**, *763*, 139568. [CrossRef]
40. Bhatia, Y.; Zheng, L.; Steinbach, L.; Günther, A.; Schneider, A.; Roth, B. Low-Cost Scalable Fabrication of Functionalized Optical Waveguide Arrays for Gas Sensing Application. *Int. J. Adv. Manuf. Technol.* **2025**, *138*, 617–633. [CrossRef]
41. Díez-Sierra, J.; Martínez, A.; Etxarri, I.; Azpitarte, I.; Pozo, B.; Quintana, I. Manufacturing Smart Surfaces with Embedded Sensors via Magnetron Sputtering and Laser Scribing. *Appl. Surf. Sci.* **2022**, *606*, 154844. [CrossRef]
42. Plogmeyer, M.; González, G.; Pongratz, C.; Schott, A.; Schulze, V.; Bräuer, G. Tool-Integrated Thin-Film Sensor Systems for Measurement of Cutting Forces and Temperatures during Machining. *Prod. Eng.* **2024**, *18*, 207–217. [CrossRef]
43. Langat, R.K.; De Luycker, E.; Cantarel, A.; Rakotondrabe, M. Integration Technology with Thin Films Co-Fabricated in Laminated Composite Structures for Defect Detection and Damage Monitoring. *Micromachines* **2024**, *15*, 274. [CrossRef] [PubMed]
44. Wu, Y.; Sicard, B.; Gadsden, S.A. Physics-Informed Machine Learning: A Comprehensive Review on Applications in Anomaly Detection and Condition Monitoring. *Expert Syst. Appl.* **2024**, *255*, 124678. [CrossRef]
45. Kushwaha, A.; Kumar, R.; Goel, N. Chemiresistive Gas Sensors beyond Metal Oxides: Using Ultrathin Two-Dimensional Nanomaterials. *FlatChem* **2024**, *43*, 100584. [CrossRef]
46. Ponzoni, A. Metal Oxide Chemiresistors: A Structural and Functional Comparison between Nanowires and Nanoparticles. *Sensors* **2022**, *22*, 3351. [CrossRef]

47. Huang, P.; Cai, Y.; Jia, Q.; Yang, Y.; Yue, T.; Zhong, S. High-Performance Piezoresistive Sensor Based on Indium Tin Oxide Nanoparticles/Cellulose Nanofiber Composite for Human Activity Monitoring. *Compos. Commun.* **2025**, *59*, 102544. [CrossRef]
48. Yin, F.; Niu, H.; Kim, E.-S.; Shin, Y.K.; Li, Y.; Kim, N.-Y. Advanced Polymer Materials-Based Electronic Skins for Tactile and Non-Contact Sensing Applications. *InfoMat* **2023**, *5*, e12424. [CrossRef]
49. Yang, Z.; Yu, X.; Song, Y.; Hu, Y.; Yang, Q.; Xiong, C.; Shi, Z. Flexible and Ultrasensitive Piezoresistive Electronic Skin Based on Chitin/Sulfonated Carbon Nanotube Films. *Int. J. Biol. Macromol.* **2024**, *259*, 129103. [CrossRef]
50. García-Martínez, J.-M.; Collar, E.P. Current and Future Insights in Organic–Inorganic Hybrid Materials. *Polymers* **2024**, *16*, 3043. [CrossRef]
51. Li, Z.; Mi, B.; Ma, X.; Liu, P.; Ma, F.; Zhang, K.; Chen, X.; Li, W. Review of Thin-Film Resistor Sensors: Exploring Materials, Classification, and Preparation Techniques. *Chem. Eng. J.* **2023**, *477*, 147029. [CrossRef]
52. Wang, S.; Kang, Y.; Wang, L.; Zhang, H.; Wang, Y.; Wang, Y. Organic/Inorganic Hybrid Sensors: A Review. *Sens. Actuators B Chem.* **2013**, *182*, 467–481. [CrossRef]
53. Zhou, B.; Yan, D. Glassy Inorganic-Organic Hybrid Materials for Photonic Applications. *Matter* **2024**, *7*, 1950–1976. [CrossRef]
54. Picelli, L.; van Veldhoven, P.J.; Verhagen, E.; Fiore, A. Hybrid Electronic–Photonic Sensors on a Fibre Tip. *Nat. Nanotechnol.* **2023**, *18*, 1162–1167. [CrossRef] [PubMed]
55. Prosa, M.; Bolognesi, M.; Fornasari, L.; Grasso, G.; Lopez-Sanchez, L.; Marabelli, F.; Toffanin, S. Nanostructured Organic/Hybrid Materials and Components in Miniaturized Optical and Chemical Sensors. *Nanomaterials* **2020**, *10*, 480. [CrossRef]
56. Gilmer, G.H.; Huang, H.; Roland, C. Thin Film Deposition: Fundamentals and Modeling. *Comput. Mater. Sci.* **1998**, *12*, 354–380. [CrossRef]
57. Poenar, D.P.; Wolffenbuttel, R.F. Thin-Film Optical Sensors with Silicon-Compatible Materials. *Appl. Opt.* **1997**, *36*, 5109–5121. [CrossRef]
58. Awan, T.I.; Afsheen, S.; Kausar, S. Fundamentals of Thin Film. In *Thin Film Deposition Techniques: Thin Film Deposition Techniques and Its Applications in Different Fields*; Awan, T.I., Afsheen, S., Kausar, S., Eds.; Springer Nature: Singapore, 2025; pp. 1–29, ISBN 978-981-96-1364-9.
59. Bailey, R.C.; Parpia, M.; Hupp, J.T. Sensing via Optical Interference. *Mater. Today* **2005**, *8*, 46–52. [CrossRef]
60. Chang, Y.; Guo, Y.; Zhao, Y. Direct and Inverse Scattering in an Optical Waveguide. *Inverse Probl.* **2024**, *40*, 125010. [CrossRef]
61. Zhou, X.; Liu, L.; Xu, W.; Song, B.; Sheng, J.; He, M.; Shi, H. A Reusable Evanescent Wave Immunosensor for Highly Sensitive Detection of Bisphenol A in Water Samples. *Sci. Rep.* **2014**, *4*, 4572. [CrossRef]
62. Joy, N.A.; Rogers, P.H.; Nandasiri, M.I.; Thevuthasan, S.; Carpenter, M.A. Plasmonic-Based Sensing Using an Array of Au–Metal Oxide Thin Films. *Anal. Chem.* **2012**, *84*, 10437–10444. [CrossRef]
63. Andam, N.; Refki, S.; Hayashi, S.; Sekkat, Z. Plasmonic Mode Coupling and Thin Film Sensing in Metal–Insulator–Metal Structures. *Sci. Rep.* **2021**, *11*, 15093. [CrossRef] [PubMed]
64. Villa, F.; Regalado, L.E.; Ramos-Mendieta, F.; Gaspar-Armenta, J.; Lopez-Ríos, T. Photonic Crystal Sensor Based on Surface Waves for Thin-Film Characterization. *Opt. Lett.* **2002**, *27*, 646–648. [CrossRef]
65. Sabarinathan, J.; Bakhtazad, A.; Poulsen, B.; Zylstra, M. Photonic Crystal Thin-Film Micro-Pressure Sensors. *J. Phys. Conf. Ser.* **2015**, *619*, 012020. [CrossRef]
66. Christensen, A.; Reynaud, M.; Posadas, A.B.; Zhan, X.; Warner, J.H.; Demkov, A.A. Electro-Optic Effect in Thin Film Strontium Barium Niobate (SBN) Grown by RF Magnetron Sputtering on SrTiO3 Substrates. *J. Appl. Phys.* **2024**, *136*, 013102. [CrossRef]
67. Säynätjoki, A.; Karvonen, L.; Alasaarela, T.; Tu, X.; Liow, T.Y.; Hiltunen, M.; Tervonen, A.; Lo, G.Q.; Honkanen, S. Low-Loss Silicon Slot Waveguides and Couplers Fabricated with Optical Lithography and Atomic Layer Deposition. *Opt. Express* **2011**, *19*, 26275–26282. [CrossRef]
68. Alasaarela, T.; Korn, D.; Alloatti, L.; Säynätjoki, A.; Tervonen, A.; Palmer, R.; Leuthold, J.; Freude, W.; Honkanen, S. Reduced Propagation Loss in Silicon Strip and Slot Waveguides Coated by Atomic Layer Deposition. *Opt. Express* **2011**, *19*, 11529–11538. [CrossRef]
69. Karasinski, P.; Zieba, M.; Gondek, E.; Niziol, J.; Gorantla, S.; Rola, K.; Bachmatiuk, A.; Tyszkiewicz, C. Sol-Gel Derived Silica-Titania Waveguide Films for Applications in Evanescent Wave Sensors—Comprehensive Study. *Materials* **2022**, *15*, 7641. [CrossRef]
70. Lv, R.; Chen, Z.; Liu, S.; Wang, J.; Li, Y.; Wang, Y.; Wang, Y. Optical Properties and Applications of Molybdenum Disulfide/SiO_2 Saturable Absorber Fabricated by Sol-Gel Technique. *Opt. Express* **2019**, *27*, 6348–6356. [CrossRef] [PubMed]
71. Butt, M.A.; Tyszkiewicz, C.; Karasiński, P.; Zięba, M.; Kaźmierczak, A.; Zdończyk, M.; Duda, Ł.; Guzik, M.; Olszewski, J.; Martynkien, T.; et al. Optical Thin Films Fabrication Techniques—Towards a Low-Cost Solution for the Integrated Photonic Platform: A Review of the Current Status. *Materials* **2022**, *15*, 4591. [CrossRef] [PubMed]
72. Zhang, Y.; Zhang, L.; Zhou, C. Review of Chemical Vapor Deposition of Graphene and Related Applications. *Acc. Chem. Res.* **2013**, *46*, 2329–2339. [CrossRef] [PubMed]

73. Wilkinson, N.J.; Smith, M.A.A.; Kay, R.W.; Harris, R.A. A Review of Aerosol Jet Printing—A Non-Traditional Hybrid Process for Micro-Manufacturing. *Int. J. Adv. Manuf. Technol.* **2019**, *105*, 4599–4619. [CrossRef]
74. Fisher, C.; Skolrood, L.N.; Li, K.; Joshi, P.C.; Aytug, T. Aerosol-Jet Printed Sensors for Environmental, Safety, and Health Monitoring: A Review. *Adv. Mater. Technol.* **2023**, *8*, 2300030. [CrossRef]
75. Clifford, B.; Beynon, D.; Phillips, C.; Deganello, D. Printed-Sensor-on-Chip Devices—Aerosol Jet Deposition of Thin Film Relative Humidity Sensors onto Packaged Integrated Circuits. *Sens. Actuators B Chem.* **2018**, *255*, 1031–1038. [CrossRef]
76. Baptista, A.; Silva, F.J.G.; Porteiro, J.; Míguez, J.L.; Pinto, G.; Fernandes, L. On the Physical Vapour Deposition (PVD): Evolution of Magnetron Sputtering Processes for Industrial Applications. *Procedia Manuf.* **2018**, *17*, 746–757. [CrossRef]
77. Borowski, P.; Myśliwiec, J. Recent Advances in Magnetron Sputtering: From Fundamentals to Industrial Applications. *Coatings* **2025**, *15*, 922. [CrossRef]
78. George, S.M. Atomic Layer Deposition: An Overview. *Chem. Rev.* **2010**, *110*, 111–131. [CrossRef]
79. Li, J.; Chai, G.; Wang, X. Atomic Layer Deposition of Thin Films: From a Chemistry Perspective. *Int. J. Extreme Manuf.* **2023**, *5*, 032003. [CrossRef]
80. Franz, G. Plasma Enhanced Chemical Vapor Deposition of Organic Polymers. *Processes* **2021**, *9*, 980. [CrossRef]
81. Singh, B.; Fischer, T.; Mathur, S. Field-Enhanced Chemical Vapor Deposition: New Perspectives for Thin Film Growth. *J. Mater. Chem. A* **2025**, *13*, 20104–20142. [CrossRef]
82. Subasri, R.; Soma Raju, K.R.C.; Samba Sivudu, K. 12-Applications of Sol–Gel Coatings: Past, Present, and Future. In *Handbook of Modern Coating Technologies*; Aliofkhazraei, M., Ali, N., Chipara, M., Bensaada Laidani, N., De Hosson, J.T.M., Eds.; Elsevier: Amsterdam, The Netherlands, 2021; pp. 425–451, ISBN 978-0-444-63237-1.
83. Werum, K.; Mueller, E.; Keck, J.; Jaeger, J.; Horter, T.; Glaeser, K.; Buschkamp, S.; Barth, M.; Eberhardt, W.; Zimmermann, A. Aerosol Jet Printing and Interconnection Technologies on Additive Manufactured Substrates. *J. Manuf. Mater. Process.* **2022**, *6*, 119. [CrossRef]
84. Valayil Varghese, T.; Eixenberger, J.; Rajabi-Kouchi, F.; Lazouskaya, M.; Francis, C.; Burgoyne, H.; Wada, K.; Subbaraman, H.; Estrada, D. Multijet Gold Nanoparticle Inks for Additive Manufacturing of Printed and Wearable Electronics. *ACS Mater. Au* **2024**, *4*, 65–73. [CrossRef]
85. Kazanskiy, N.L.; Khorin, P.A.; Khonina, S.N. Biochips on the Move: Emerging Trends in Wearable and Implantable Lab-on-Chip Health Monitors. *Electronics* **2025**, *14*, 3224. [CrossRef]
86. Heckingbottom, R.; Todd, C.J.; Davies, G.J. The Interplay of Thermodynamics and Kinetics in Molecular Beam Epitaxy (MBE) of Doped Gallium Arsenide. *J. Electrochem. Soc.* **1980**, *127*, 444. [CrossRef]
87. Asahi, H.; Horikoshi, Y. General Description of MBE. In *Molecular Beam Epitaxy: Materials and Applications for Electronics and Optoelectronics*; Wiley: Hoboken, NJ, USA, 2019; pp. 23–39, ISBN 978-1-119-35500-7.
88. Farrow, R.F.C.; Harp, G.R.; Weller, D.K.; Marks, R.F.; Toney, M.F.; Cebollada, A.; Rabedeau, T.A. Molecular-Beam Epitaxy (MBE) Growth of Chemically Ordered Co-Pt and Fe-Pt Alloy Phases. In *Proceedings of the Epitaxial Growth Processes*; SPIE: Bellingham, WA, USA, 1994; Volume 2140, pp. 106–111.
89. Butt, M.A. Integrated Optics: Platforms and Fabrication Methods. *Encyclopedia* **2023**, *3*, 824–838. [CrossRef]
90. Cognetti, J.S.; Moen, M.T.; Brewer, M.G.; Bryan, M.R.; Tice, J.D.; McGrath, J.L.; Miller, B.L. A Photonic Biosensor-Integrated Tissue Chip Platform for Real-Time Sensing of Lung Epithelial Inflammatory Markers. *Lab Chip* **2023**, *23*, 239–250. [CrossRef]
91. Kazanskiy, N.L.; Oseledets, I.V.; Nikonorov, A.V.; Chertykovtseva, V.O.; Khonina, S.N. Exploring the Frontier of Integrated Photonic Logic Gates: Breakthrough Designs and Promising Applications. *Technologies* **2025**, *13*, 314. [CrossRef]
92. Jin, C.; Zhou, J.; Wu, Z.; Zhang, J.X.J. Doped Zinc Oxide-Based Piezoelectric Devices for Energy Harvesting and Sensing. *Adv. Energy Sustain. Res.* **2025**, *6*, 2500017. [CrossRef]
93. Balasubramanian, K.; Han, X.F.; Guenther, K.H. Comparative Study of Titanium Dioxide Thin Films Produced by Electron-Beam Evaporation and by Reactive Low-Voltage Ion Plating. *Appl. Opt.* **1993**, *32*, 5594–5600. [CrossRef]
94. Kong, Y.; Li, Y.; Cui, X.; Su, L.; Ma, D.; Lai, T.; Yao, L.; Xiao, X.; Wang, Y. SnO_2 Nanostructured Materials Used as Gas Sensors for the Detection of Hazardous and Flammable Gases: A Review. *Nano Mater. Sci.* **2022**, *4*, 339–350. [CrossRef]
95. Gao, C.; Guo, X.; Nie, L.; Wu, X.; Peng, L.; Chen, J. A Review on WO_3 Gasochromic Film: Mechanism, Preparation and Properties. *Int. J. Hydrogen Energy* **2023**, *48*, 2442–2465. [CrossRef]
96. Szafraniak, B.; Fuśnik, Ł.; Xu, J.; Gao, F.; Brudnik, A.; Rydosz, A. Semiconducting Metal Oxides: SrTiO3, BaTiO3 and BaSrTiO3 in Gas-Sensing Applications: A Review. *Coatings* **2021**, *11*, 185. [CrossRef]
97. Mansour, C.; Benwadih, M.; Revenant, C. Sol–Gel Derived Barium Strontium Titanate Thin Films Using a Highly Diluted Precursor Solution. *AIP Adv.* **2021**, *11*, 085302. [CrossRef]
98. Arefnia, F.; Zibaii, M.I.; Layeghi, A.; Rostami, S.; Babakhani-Fard, M.-M.; Moghadam, F.M. Citrate Polymer Optical Fiber for Measuring Refractive Index Based on LSPR Sensor. *Sci. Rep.* **2024**, *14*, 18637. [CrossRef]
99. Baburin, A.S.; Merzlikin, A.M.; Baryshev, A.V.; Ryzhikov, I.A.; Panfilov, Y.V.; Rodionov, I.A. Silver-Based Plasmonics: Golden Material Platform and Application Challenges [Invited]. *Opt. Mater. Express* **2019**, *9*, 611–642. [CrossRef]

100. Campos, A.; Troc, N.; Cottancin, E.; Pellarin, M.; Weissker, H.-C.; Lermé, J.; Kociak, M.; Hillenkamp, M. Plasmonic Quantum Size Effects in Silver Nanoparticles Are Dominated by Interfaces and Local Environments. *Nat. Phys.* **2019**, *15*, 275–280. [CrossRef]
101. Nur'aini, A.; Oh, I. Volatile Organic Compound Gas Sensors Based on Methylammonium Lead Iodide Perovskite Operating at Room Temperature. *RSC Adv.* **2020**, *10*, 12982–12987. [CrossRef] [PubMed]
102. Patel, M.R.; Singh, P.D.D.; Harshita; Basu, H.; Choi, Y.; Murthy, Z.V.P.; Park, T.J.; Kailasa, S.K. Single Crystal Perovskites: Synthetic Strategies, Properties and Applications in Sensing, Detectors, Solar Cells and Energy Storage Devices. *Coord. Chem. Rev.* **2024**, *519*, 216105. [CrossRef]
103. Li, L.; Liu, J.; Zeng, M.; Fu, L. Space-Confined Growth of Metal Halide Perovskite Crystal Films. *Nano Res.* **2021**, *14*, 1609–1624. [CrossRef]
104. Demontis, V.; Durante, O.; Marongiu, D.; De Stefano, S.; Matta, S.; Simbula, A.; Ragazzo Capello, C.; Pennelli, G.; Quochi, F.; Saba, M.; et al. Photoconduction in 2D Single-Crystal Hybrid Perovskites. *Adv. Opt. Mater.* **2025**, *13*, 2402469. [CrossRef]
105. Butt, M.A. Beyond the Detection Limit: A Review of High-Q Optical Ring Resonator Sensors. *Mater. Today Phys.* **2025**, *58*, 101873. [CrossRef]
106. Chen, L.-Y.; Chen, Y.-J.; Wu, D.-S.; Huang, W.-H.; Wang, C.-T. High-Sensitivity Silicon Nitride Optical Temperature Sensor Based on Cascaded Mach-Zehnder Interferometers. *Opt. Mater.* **2025**, *165*, 117139. [CrossRef]
107. Datta-Chaudhuri, T.; Abshire, P.; Smela, E. Packaging Commercial CMOS Chips for Lab on a Chip Integration. *Lab Chip* **2014**, *14*, 1753–1766. [CrossRef]
108. Bonopera, M. Fiber-Bragg-Grating-Based Displacement Sensors: Review of Recent Advances. *Materials* **2022**, *15*, 5561. [CrossRef] [PubMed]
109. Li, H.-C.; Leng, Y.-K.; Liao, Y.-C.; Liu, B.; Luo, W.; Liu, J.; Shi, J.-L.; Yuan, J.; Xu, H.-Y.; Xiong, Y.-H.; et al. Tapered Microfiber MZI Biosensor for Highly Sensitive Detection of Staphylococcus Aureus. *IEEE Sens. J.* **2022**, *22*, 5531–5539. [CrossRef]
110. Getahun Kumela, A.; Belay Gemta, A.; Kebede Hordofa, A.; Birhanu, R.; Dagnaw Mekonnen, H.; Sherefedin, U.; Weldegiorgis, K. A Review on Hybridization of Plasmonic and Photonic Crystal Biosensors for Effective Cancer Cell Diagnosis. *Nanoscale Adv.* **2023**, *5*, 6382–6399. [CrossRef]
111. Tan, J.; Chen, Y.; He, J.; Occhipinti, L.G.; Wang, Z.; Zhou, X. Two-Dimensional Material-Enhanced Surface Plasmon Resonance for Antibiotic Sensing. *J. Hazard. Mater.* **2023**, *455*, 131644. [CrossRef]
112. Hu, M.; Li, M.; Li, M.-Y.; Wen, X.; Deng, S.; Liu, S.; Lu, H. Sensitivity Enhancement of 2D Material-Based Surface Plasmon Resonance Sensor with an Al–Ni Bimetallic Structure. *Sensors* **2023**, *23*, 1714. [CrossRef]
113. Weiss, R.; Diehl, M.; Reuter, J. Predictive Temperature Control of an Industrial Heating Process. *IFAC-Pap.* **2024**, *58*, 107–112. [CrossRef]
114. Baciu, A.; Lazar, C. Model-Free Temperature Control of Heat Treatment Process. *Energies* **2024**, *17*, 3679. [CrossRef]
115. Butt, M.A. Emerging Trends in Thermo-Optic and Electro-Optic Materials for Tunable Photonic Devices. *Materials* **2025**, *18*, 2782. [CrossRef]
116. Larciprete, M.C.; Centini, M.; Paoloni, S.; Fratoddi, I.; Dereshgi, S.A.; Tang, K.; Wu, J.; Aydin, K. Adaptive Tuning of Infrared Emission Using VO_2 Thin Films. *Sci. Rep.* **2020**, *10*, 11544. [CrossRef]
117. Welsch, E.; Ristau, D. Photothermal Measurements on Optical Thin Films. *Appl. Opt.* **1995**, *34*, 7239–7253. [CrossRef] [PubMed]
118. Rashed, A.N.Z.; Zaky, M.M.; Mohamed, A.E.-N.A.; Ahmed, H.E.H.; Elsaket, A.I. Applications of an Extremely Sensitive Temperature Sensor Based on Surface Plasmon Photonic Crystal Fiber in Nuclear Reactors. *J. Opt.* **2025**. [CrossRef]
119. Tyler Gates, J.; Tsvetkov, P.V. Testing of Fiber Optic Based Sensors for Advanced Reactors in the Texas A&M University TRIGA Reactor. *Ann. Nucl. Energy* **2024**, *196*, 110222. [CrossRef]
120. Chen, Q.; Qiang, D.; Lin, J.; Jia, S.; Xu, L.; Ye, E.; Jiang, W.; Li, H.; Sun, D. Polymer-Derived Ceramics Phosphor Thin-Film Sensors for Extreme Environment. *Ceram. Int.* **2025**, *51*, 38990–39001. [CrossRef]
121. He, G.; He, Y.; Xu, L.; Li, L.; Wang, L.; Hai, Z.; Sun, D. La(Ca)CrO_3-Filled SiCN Precursor Thin Film Temperature Sensor Capable to Measure up to 1100 °C High Temperature. *Micromachines* **2023**, *14*, 1719. [CrossRef] [PubMed]
122. Aslanidis, E.; Skotadis, E.; Moutoulas, E.; Tsoukalas, D. Thin Film Protected Flexible Nanoparticle Strain Sensors: Experiments and Modeling. *Sensors* **2020**, *20*, 2584. [CrossRef]
123. Maciak, E. Low-Coherence Interferometric Fiber Optic Sensor for Humidity Monitoring Based on Nafion® Thin Film. *Sensors* **2019**, *19*, 629. [CrossRef]
124. Bartnik, K.; Martychowiec, A.; Kwietniewski, N.; Musolf, P.; Niedziółka-Jönsson, J.; Koba, M.; Śmietana, M. Thin-Film-Based Optical Fiber Interferometric Sensor on the Fiber Tip for Endovascular Surgical Procedures. *IEEE Trans. Biomed. Eng.* **2025**, *72*, 930–939. [CrossRef]
125. Jiang, M.; Gerhard, E. A Simple Strain Sensor Using a Thin Film as a Low-Finesse Fiber-Optic Fabry–Perot Interferometer. *Sens. Actuators Phys.* **2001**, *88*, 41–46. [CrossRef]
126. Ali, O. Revolutionizing Infrastructure: The Future of Fiber Optic Sensing in Structural Health Monitoring. Available online: https://www.azooptics.com/Article.aspx?ArticleID=2572 (accessed on 23 April 2025).

127. Butt, M.A. A Comprehensive Exploration of Contemporary Photonic Devices in Space Exploration: A Review. *Photonics* **2024**, *11*, 873. [CrossRef]
128. Yokota, T.; Zalar, P.; Kaltenbrunner, M.; Jinno, H.; Matsuhisa, N.; Kitanosako, H.; Tachibana, Y.; Yukita, W.; Koizumi, M.; Someya, T. Ultraflexible Organic Photonic Skin. *Sci. Adv.* **2016**, *2*, e1501856. [CrossRef]
129. Occhialini, C.A.; Martins, L.G.P.; Fan, S.; Bisogni, V.; Yasunami, T.; Musashi, M.; Kawasaki, M.; Uchida, M.; Comin, R.; Pelliciari, J. Strain-Modulated Anisotropic Electronic Structure in Superconducting RuO_2 Films. *Phys. Rev. Mater.* **2022**, *6*, 084802. [CrossRef]
130. Wong, F.J.; Baek, S.-H.; Chopdekar, R.V.; Mehta, V.V.; Jang, H.-W.; Eom, C.-B.; Suzuki, Y. Metallicity in $LaTiO_3$ Thin Films Induced by Lattice Deformation. *Phys. Rev. B* **2010**, *81*, 161101. [CrossRef]
131. Mishra, R.K.; Verma, K.; singh, D. sethi Defect Engineering in Nanomaterials: Impact, Challenges, and Applications. *Smart Mater. Manuf.* **2024**, *2*, 100052. [CrossRef]
132. Yaqoob, U.; Younis, M.I. Chemical Gas Sensors: Recent Developments, Challenges, and the Potential of Machine Learning—A Review. *Sensors* **2021**, *21*, 2877. [CrossRef]
133. Waqas Alam, M.; Sharma, A.; Sharma, A.; Kumar, S.; Mohammad Junaid, P.; Awad, M. VOC Detection with Zinc Oxide Gas Sensors: A Review of Fabrication, Performance, and Emerging Applications. *Electroanalysis* **2025**, *37*, e202400246. [CrossRef]
134. Mazur, M.; Kapuścik, P.; Weichbrodt, W.; Domaradzki, J.; Mazur, P.; Kot, M.; Flege, J.I. WO_3 Thin-Film Optical Gas Sensors Based on Gasochromic Effect towards Low Hydrogen Concentrations. *Materials* **2023**, *16*, 3831. [CrossRef] [PubMed]
135. Wang, Y. Application of Graphene as Sensors: A Review. *J. Phys. Conf. Ser.* **2023**, *2608*, 012022. [CrossRef]
136. An, N.; Qin, C.; Li, Y.; Tan, T.; Yuan, Z.; Zhang, H.; Wu, Y.; Yao, B.; Rao, Y. Graphene-Fiber Biochemical Sensors: Principles, Implementations, and Advances. *Photonic Sens.* **2021**, *11*, 123–139. [CrossRef]
137. Bado, M.F.; Casas, J.R. A Review of Recent Distributed Optical Fiber Sensors Applications for Civil Engineering Structural Health Monitoring. *Sensors* **2021**, *21*, 1818. [CrossRef]
138. Prasanth, A.; Meher, S.R.; Alex, Z.C. Metal Oxide Thin Films Coated Evanescent Wave Based Fiber Optic VOC Sensor. *Sens. Actuators Phys.* **2022**, *338*, 113459. [CrossRef]
139. Yun, C.-Y.; Dhital, D.; Lee, J.-R.; Park, G.; Kwon, I.-B. Design of Multiplexed Fiber Optic Chemical Sensing System Using Clad-Removable Optical Fibers. *Opt. Laser Technol.* **2012**, *44*, 269–280. [CrossRef]
140. Motala, M.; Beagle, L.K.; Lynch, J.; Moore, D.C.; Stevenson, P.R.; Benton, A.; Tran, L.D.; Baldwin, L.A.; Austin, D.; Muratore, C.; et al. Selective Vapor Sensors with Thin-Film MoS_2-Coated Optical Fibers. *J. Vac. Sci. Technol. A* **2022**, *40*, 032202. [CrossRef]
141. Sapkota, R.; Duan, P.; Kumar, T.; Venkataraman, A.; Papadopoulos, C. Thin Film Gas Sensors Based on Planetary Ball-Milled Zinc Oxide Nanoinks: Effect of Milling Parameters on Sensing Performance. *Appl. Sci.* **2021**, *11*, 9676. [CrossRef]
142. Ali, M.; Ahmad, I.; Geun, I.; Hamza, S.A.; Ijaz, U.; Jang, Y.; Koo, J.; Kim, Y.-G.; Kim, H.-D. A Comprehensive Review of Advanced Sensor Technologies for Fire Detection with a Focus on Gasistor-Based Sensors. *Chemosensors* **2025**, *13*, 230. [CrossRef]
143. Butt, M.A.; Piramidowicz, R. Integrated Photonic Sensors for the Detection of Toxic Gasses—A Review. *Chemosensors* **2024**, *12*, 143. [CrossRef]
144. Korotchenkov, G.; Brynzari, V.; Dmitriev, S. SnO2 Thin Film Gas Sensors for Fire-Alarm Systems. *Sens. Actuators B Chem.* **1999**, *54*, 191–196. [CrossRef]
145. Antonacci, G.; Goyvaerts, J.; Zhao, H.; Baumgartner, B.; Lendl, B.; Baets, R. Ultra-Sensitive Refractive Index Gas Sensor with Functionalized Silicon Nitride Photonic Circuits. *APL Photonics* **2020**, *5*, 081301. [CrossRef]
146. Zhang, Q.; Liu, Y.; Li, H.; Wang, J.; Wang, Y.; Cheng, F.; Han, H.; Zhang, P. A Review of SiC Sensor Applications in High-Temperature and Radiation Extreme Environments. *Sensors* **2024**, *24*, 7731. [CrossRef]
147. Berwal, P.; Rani, S.; Sihag, S.; Singh, P.; Bulla, M.; Jatrana, A.; Kumar, A.; Kumar, A.; Kumar, V. Fabrication of NiO Based Thin Film for High-Performance NO_2 Gas Sensors at Low Concentrations. *Phys. B Condens. Matter* **2024**, *685*, 416023. [CrossRef]
148. Escobedo, P.; Fernández-Ramos, M.D.; López-Ruiz, N.; Moyano-Rodríguez, O.; Martínez-Olmos, A.; Pérez de Vargas-Sansalvador, I.M.; Carvajal, M.A.; Capitán-Vallvey, L.F.; Palma, A.J. Smart Facemask for Wireless CO_2 Monitoring. *Nat. Commun.* **2022**, *13*, 72. [CrossRef]
149. Ricci, P.P.; Gregory, O.J. Free-Standing, Thin-Film Sensors for the Trace Detection of Explosives. *Sci. Rep.* **2021**, *11*, 6623. [CrossRef]
150. Ramírez-García, G.; Wang, L.; Yetisen, A.K.; Morales-Narváez, E. Photonic Solutions for Challenges in Sensing. *ACS Omega* **2024**, *9*, 25415–25420. [CrossRef]
151. Liu, Y.; Liu, Q.; Chen, S.; Cheng, F.; Wang, H.; Peng, W. Surface Plasmon Resonance Biosensor Based on Smart Phone Platforms. *Sci. Rep.* **2015**, *5*, 12864. [CrossRef]
152. Ma, C.; Peng, D.; Bai, X.; Liu, S.; Luo, L. A Review of Optical Fiber Sensing Technology Based on Thin Film and Fabry–Perot Cavity. *Coatings* **2023**, *13*, 1277. [CrossRef]
153. Singh, S.; Chaudhary, B.; Upadhyay, A.; Sharma, D.; Ayyanar, N.; Taya, S.A. A Review on Various Sensing Prospects of SPR Based Photonic Crystal Fibers. *Photonics Nanostructures-Fundam. Appl.* **2023**, *54*, 101119. [CrossRef]
154. Yang, M.; Dai, J. Review on Optical Fiber Sensors with Sensitive Thin Films. *Photonic Sens.* **2012**, *2*, 14–28. [CrossRef]

155. Meyer-Kornblum, E.; Biehl, S.; Paetsch, N.; Bräuer, G. Investigation of Application-Specific Thin Film Sensor Systems with Wireless Data Transmission System. *Proceedings* **2018**, *2*, 919. [CrossRef]
156. Tang, X.; Wang, X.; Cattley, R.; Gu, F.; Ball, A.D. Energy Harvesting Technologies for Achieving Self-Powered Wireless Sensor Networks in Machine Condition Monitoring: A Review. *Sensors* **2018**, *18*, 4113. [CrossRef] [PubMed]
157. Hsiao, C.N.; Chen, H.P.; Chiu, P.K.; Cho, W.H.; Lin, Y.W.; Chen, F.Z.; Tsai, D.P. Design and Fabrication of Optical Thin Films for Remote Sensing Instruments. *J. Vac. Sci. Technol. A* **2010**, *28*, 867–872. [CrossRef]
158. Song, Q.; Xu, X.; Zi, J.; Wang, J.; Peng, Z.; Zhang, B.; Zhang, M. A High-Performance Thin-Film Sensor in 6G for Remote Sensing of the Sea Surface. *Remote Sens.* **2023**, *15*, 3682. [CrossRef]
159. Liu, Z.; Tian, B.; Zhang, B.; Liu, J.; Zhang, Z.; Wang, S.; Luo, Y.; Zhao, L.; Shi, P.; Lin, Q.; et al. A Thin-Film Temperature Sensor Based on a Flexible Electrode and Substrate. *Microsyst. Nanoeng.* **2021**, *7*, 42. [CrossRef]
160. Bernabé, S.; Tekin, T.; Sirbu, B.; Charbonnier, J.; Grosse, P.; Seyfried, M. Packaging and Test of Photonic Integrated Circuits (PICs). In *Integrated Nanophotonics*; John Wiley & Sons, Ltd.: Hoboken, NJ, USA, 2023; pp. 1–52, ISBN 978-3-527-83303-0.
161. Caballero, L.P.; Povinelli, M.L.; Ramirez, J.C.; Guimarães, P.S.S.; Neto, O.P.V. Photonic Crystal Integrated Logic Gates and Circuits. *Opt. Express* **2022**, *30*, 1976–1993. [CrossRef]
162. Butt, M.A.; Słowikowski, M.; Drecka, D.; Jarosik, M.; Piramidowicz, R. Experimental Characterization of a Silicon Nitride Asymmetric Loop-Terminated Mach-Zehnder Interferometer with a Refractive Index-Engineered Sensing Arm. *Nanomaterials* **2025**, *15*, 1532. [CrossRef] [PubMed]
163. Muellner, P.; Bruck, R.; Baus, M.; Karl, M.; Wahlbrink, T.; Hainberger, R. On-Chip Multiplexing Concept for Silicon Photonic MZI Biosensor Array. *Proc. SPIE-Int. Soc. Opt. Eng.* **2012**, *8431*, 18. [CrossRef]
164. Taharat, A.; Kabir, M.A.; Keats, A.I.; Rakib, A.K.M.; Sagor, R.H. Advancing Optomechanical Sensing: Novel CMOS-Compatible Plasmonic Pressure Sensor with Silicon-Insulator-Silicon Waveguide Configuration. *Opt. Commun.* **2025**, *578*, 131495. [CrossRef]
165. Augel, L.; Kawaguchi, Y.; Bechler, S.; Körner, R.; Schulze, J.; Uchida, H.; Fischer, I.A. Integrated Collinear Refractive Index Sensor with Ge PIN Photodiodes. *ACS Photonics* **2018**, *5*, 4586–4593. [CrossRef]
166. Saha, S.; Dutta, A.; Kinsey, N.; Kildishev, A.V.; Shalaev, V.M.; Boltasseva, A. On-Chip Hybrid Photonic-Plasmonic Waveguides with Ultrathin Titanium Nitride Films. *ACS Photonics* **2018**, *5*, 4423–4431. [CrossRef]
167. Li, X.; Pei, W.; Lu, Y.; Li, W.; Huang, A.; Jiao, H.; Feng, D.; Zhou, Z.; Feng, L. Thin-Film Lithium Niobate Multi-Channel Multifunctional Photonic Integrated Chip for Interferometric Optical Gyroscope. *Opt. Express* **2025**, *33*, 30669–30685. [CrossRef]
168. Wrbanek, J.D.; Fralick, G.C. Thin Film Physical Sensors for High Temperature Applications. In Proceedings of the NASA-GE Instrumentation Mini Workshop, Cleveland, OH, USA, 22 October 2020.
169. Nadafan, M.; Shahram, S.; Zamir Anvari, J.; Khashehchi, M. Thermal and Optical Characterization of a Resistance-Temperature Detector Based on Platinum Thin Film: Design and Fabrication. *Optik* **2023**, *290*, 171349. [CrossRef]
170. Reddy, H.; Guler, U.; Kudyshev, Z.; Kildishev, A.V.; Shalaev, V.M.; Boltasseva, A. Temperature-Dependent Optical Properties of Plasmonic Titanium Nitride Thin Films. *ACS Photonics* **2017**, *4*, 1413–1420. [CrossRef]
171. Tien, C.-L.; Chiang, C.-Y.; Wang, C.-C.; Lin, S.-C. Temperature-Dependent Residual Stresses and Thermal Expansion Coefficient of VO2 Thin Films. *Inventions* **2024**, *9*, 61. [CrossRef]
172. Guk, E.; Ranaweera, M.; Venkatesan, V.; Kim, J.-S. Performance and Durability of Thin Film Thermocouple Array on a Porous Electrode. *Sensors* **2016**, *16*, 1329. [CrossRef] [PubMed]
173. Fang, Z.; Wu, X.; Zhao, H.; Fang, X.; Wu, C.; Zhang, D.; Zhang, Z.; Tian, B.; Zhao, L.; Li, T.; et al. Pt Thin-Film Resistance Thermo Detectors with Stable Interfaces for Potential Integration in SiC High-Temperature Pressure Sensors. *Microsyst. Nanoeng.* **2024**, *10*, 133. [CrossRef]
174. Yanguas-Gil, A.; Elam, J.W. Modeling Scale-up of Particle Coating by Atomic Layer Deposition. *J. Vac. Sci. Technol. A* **2024**, *43*, 012404. [CrossRef]
175. Joyce, B.A. Molecular Beam Epitaxy-Fundamentals and Current Status. In *Contemporary Physics*; SSMATERIALS, Volume 7; Springer: Berlin/Heidelberg, Germany, 1990. [CrossRef]
176. Jalili, S.; Hajakbari, F.; Hojabri, A. Effect of Silver Thickness on Structural, Optical and Morphological Properties of Nanocrystalline Ag/NiO Thin Films. *J. Theor. Appl. Phys.* **2018**, *12*, 15–22. [CrossRef]
177. Marques, M.J.M.; Lin, W.; Taima, T.; Umezu, S.; Shahiduzzaman, M. Unleashing the Potential of Industry Viable Roll-to-Roll Compatible Technologies for Perovskite Solar Cells: Challenges and Prospects. *Mater. Today* **2024**, *78*, 112–141. [CrossRef]
178. Bulowski, W.; Knura, R.; Socha, R.P.; Basiura, M.; Skibińska, K.; Wojnicki, M. Thin Film Semiconductor Metal Oxide Oxygen Sensors: Limitations, Challenges, and Future Progress. *Electronics* **2024**, *13*, 3409. [CrossRef]
179. Borisov, S.M.; Seifner, R.; Klimant, I. A Novel Planar Optical Sensor for Simultaneous Monitoring of Oxygen, Carbon Dioxide, pH and Temperature. *Anal. Bioanal. Chem.* **2011**, *400*, 2463–2474. [CrossRef]
180. Kanth, S.; Choudhury, S.; Kumar, S.; Rao, R.; Debnath, A.K.; Betty, C.A. Reliable NO_2 Sensing and Alert System Based on Pd-PdO Thin Film with Sub Ppm Level Detection at Room Temperature. *Sens. Actuators B Chem.* **2024**, *403*, 135145. [CrossRef]

181. Ward, S.J.; Weiss, S.M. Reducing Detection Limits of Porous Silicon Thin Film Optical Sensors Using Signal Processing. In Proceedings of the Frontiers in Biological Detection: From Nanosensors to Systems XIII, San Francisco, CA, USA, 16 March 2021; SPIE: Bellingham, WA, USA, 2021; Volume 11662, pp. 37–45.
182. Röbisch, V.; Salzer, S.; Urs, N.O.; Reermann, J.; Yarar, E.; Piorra, A.; Kirchhof, C.; Lage, E.; Höft, M.; Schmidt, G.U.; et al. Pushing the Detection Limit of Thin Film Magnetoelectric Heterostructures. *J. Mater. Res.* **2017**, *32*, 1009–1019. [CrossRef]
183. Almulla, L.; Mariello, M.; Proctor, C.M. High Dynamic Range Thin-Film Resistive Flow Sensors for Monitoring Diverse Biofluids. *Adv. Funct. Mater.* **2025**, e10372. [CrossRef]
184. Horst, D.; Scherr, H.; Lueder, E.H. Increasing the Dynamic Range of an Array of Light Sensors Using a New Thin-Film Circuit. In Proceedings of the Solid State Sensor Arrays and CCD Cameras, San Jose, CA, USA, 25 March 1996; SPIE: Bellingham, WA, USA; Volume 2654, pp. 99–107.
185. Hu, P.; Shi, Y.; Du, Q.; Feng, S.; Yang, Y.; Li, L.; Chen, K.; Xue, D. Ceramic Phosphors for Laser-Driven Lighting. *Rev. Mater. Res.* **2025**, *1*, 100092. [CrossRef]
186. Ebadi, S.M.; Khani, S.; Örtegren, J. Ultra-Compact Multifunctional Surface Plasmon Device with Tailored Optical Responses. *Results Phys.* **2024**, *61*, 107783. [CrossRef]
187. Kim, J.T.; Choi, H.; Shin, E.; Park, S.; Kim, I.G. Graphene-Based Optical Waveguide Tactile Sensor for Dynamic Response. *Sci. Rep.* **2018**, *8*, 16118. [CrossRef]
188. Alabbas, S.H.; Ashworth, D.C.; Bezzaa, B.; Momin, S.A.; Narayanaswamy, R. Factors Affectig the Response Time of an Optical-Fibre Reflectance pH Sensor. *Sens. Actuators Phys.* **1995**, *51*, 129–134. [CrossRef]
189. Barra, G.; Guadagno, L.; Raimondo, M.; Santonicola, M.G.; Toto, E.; Vecchio Ciprioti, S. A Comprehensive Review on the Thermal Stability Assessment of Polymers and Composites for Aeronautics and Space Applications. *Polymers* **2023**, *15*, 3786. [CrossRef]
190. Guan, R.; Zou, F.; Li, D.; Yao, Y. A High-Thermal-Stability, Fully Spray Coated Multilayer Thin-Film Graphene/Polyamide-Imide Nanocomposite Strain Sensor for Acquiring High-Frequency Ultrasonic Waves. *Compos. Sci. Technol.* **2022**, *227*, 109628. [CrossRef]
191. Jacobo-Martín, A.; Jost, N.; Hernández, J.J.; Domínguez, C.; Vallerotto, G.; Askins, S.; Antón, I.; Rodríguez, I. Roll-to-Roll Nanoimprint Lithography of High Efficiency Fresnel Lenses for Micro-Concentrator Photovoltaics. *Opt. Express* **2021**, *29*, 34135–34149. [CrossRef]
192. Kang, M.H.; Lee, G.J.; Yun, J.H.; Song, Y.M. NFC-Based Wearable Optoelectronics Working with Smartphone Application for Untact Healthcare. *Sensors* **2021**, *21*, 878. [CrossRef]
193. Zhou, H.; Li, D.; Lee, C. Technology Landscape Review of In-Sensor Photonic Intelligence: From Optical Sensors to Smart Devices. *AI Sens.* **2025**, *1*, 5. [CrossRef]
194. Venketeswaran, A.; Lalam, N.; Wuenschell, J.; Ohodnicki, P.R., Jr.; Badar, M.; Chen, K.P.; Lu, P.; Duan, Y.; Chorpening, B.; Buric, M. Recent Advances in Machine Learning for Fiber Optic Sensor Applications. *Adv. Intell. Syst.* **2022**, *4*, 2100067. [CrossRef]
195. Flynn, C.D.; Chang, D. Artificial Intelligence in Point-of-Care Biosensing: Challenges and Opportunities. *Diagnostics* **2024**, *14*, 1100. [CrossRef]
196. Su, Y.-D.; Ohodnicki, P.R.; Wuenschell, J.K.; Lalam, N.; Sarcinelli, E.; Buric, M.P.; Wright, R. Multiparameter Optical Fiber Sensing for Energy Infrastructure through Nanoscale Light–Matter Interactions: From Hardware to Software, Science to Commercial Opportunities. *APL Photonics* **2024**, *9*, 120902. [CrossRef]
197. Arockiyadoss, M.A.; Yao, C.-K.; Liu, P.-C.; Kumar, P.; Nagi, S.K.; Dehnaw, A.M.; Peng, P.-C. Spectral Demodulation of Mixed-Linewidth FBG Sensor Networks Using Cloud-Based Deep Learning for Land Monitoring. *Sensors* **2025**, *25*, 5627. [CrossRef]
198. Kruse, L.E.; Kühl, S.; Dochhan, A.; Pachnicke, S. Experimental Investigation of Machine-Learning-Based Soft-Failure Management Using the Optical Spectrum. *J. Opt. Commun. Netw.* **2024**, *16*, 94–103. [CrossRef]
199. Parker Tian, S.I.; Ren, Z.; Venkataraj, S.; Cheng, Y.; Bash, D.; Oviedo, F.; Senthilnath, J.; Chellappan, V.; Lim, Y.-F.; Aberle, A.G.; et al. Tackling Data Scarcity with Transfer Learning: A Case Study of Thickness Characterization from Optical Spectra of Perovskite Thin Films. *Digit. Discov.* **2023**, *2*, 1334–1346. [CrossRef]
200. Hamza, A.; Ali, Z.; Dudley, S.; Saleem, K.; Uneeb, M.; Christofides, N. A Multi-Stage Review Framework for AI-Driven Predictive Maintenance and Fault Diagnosis in Photovoltaic Systems. *Appl. Energy* **2025**, *393*, 126108. [CrossRef]
201. Ngo, D.; Park, H.-C.; Kang, B. Edge Intelligence: A Review of Deep Neural Network Inference in Resource-Limited Environments. *Electronics* **2025**, *14*, 2495. [CrossRef]
202. Kazanskiy, N.L.; Khonina, S.N.; Butt, M.A. A Review of Photonic Sensors Based on Ring Resonator Structures: Three Widely Used Platforms and Implications of Sensing Applications. *Micromachines* **2023**, *14*, 1080. [CrossRef]
203. Hawkeye, M.M.; Taschuk, M.T.; Brett, M.J. Introduction: Glancing Angle Deposition Technology. In *Glancing Angle Deposition of Thin Films: Engineering the Nanoscale*; Wiley: Hoboken, NJ, USA, 2014; pp. 1–30, ISBN 978-1-118-84732-9.
204. Pula, P.; Leniart, A.A.; Krol, J.; Gorzkowski, M.T.; Suster, M.C.; Wrobel, P.; Lewera, A.; Majewski, P.W. Block Copolymer-Templated, Single-Step Synthesis of Transition Metal Oxide Nanostructures for Sensing Applications. *ACS Appl. Mater. Interfaces* **2023**, *15*, 57970–57980. [CrossRef]

205. Cao, Y.; Ma, D.; Li, H.; Cui, G.; Zhang, J.; Yang, Z. Review of Industrialization Development of Nanoimprint Lithography Technology. *Chips* **2025**, *4*, 10. [CrossRef]
206. Luo, Y.; Abidian, M.R.; Ahn, J.-H.; Akinwande, D.; Andrews, A.M.; Antonietti, M.; Bao, Z.; Berggren, M.; Berkey, C.A.; Bettinger, C.J.; et al. Technology Roadmap for Flexible Sensors. *ACS Nano* **2023**, *17*, 5211–5295. [CrossRef] [PubMed]
207. Ben Said, L.; Ayadi, B.; Alharbi, S.; Dammak, F. Recent Advances in Additive Manufacturing: A Review of Current Developments and Future Directions. *Machines* **2025**, *13*, 813. [CrossRef]
208. He, S.; Wang, C.; Tao, J.; Tang, H.; Wang, Z.; Song, J. A Kirigami-Based Reconfigurable Metasurface for Selective Electromagnetic Transmission Modulation. *Npj Flex. Electron.* **2024**, *8*, 48. [CrossRef]
209. Dai, C.; Rho, Y.; Pham, K.; McCormick, B.; Blankenship, B.W.; Zhao, W.; Zhang, Z.; Gilbert, S.M.; Crommie, M.F.; Wang, F.; et al. Kirigami Engineering of Suspended Graphene Transducers. *Nano Lett.* **2022**, *22*, 5301–5306. [CrossRef]
210. Choi, J.; Visagie, I.; Chen, Y.; Abbel, R.; Parker, K. NFC-Enabled Dual-Channel Flexible Printed Sensor Tag. *Sensors* **2023**, *23*, 6765. [CrossRef] [PubMed]
211. Park, S.W.; Han, G.D.; Choi, H.J.; Prinz, F.B.; Shim, J.H. Evaluation of Atomic Layer Deposited Alumina as a Protective Layer for Domestic Silver Articles: Anti-Corrosion Test in Artificial Sweat. *Appl. Surf. Sci.* **2018**, *441*, 718–723. [CrossRef]
212. Pérez-López, D.; López, A.; DasMahapatra, P.; Capmany, J. Multipurpose Self-Configuration of Programmable Photonic Circuits. *Nat. Commun.* **2020**, *11*, 6359. [CrossRef]
213. Tiuftiakov, N.Y.; Kalinichev, A.V.; Gryazev, I.P.; Peshkova, M.A. Ion-Selective Optical Sensors with Internal Reference: On the Quest for Prolonged Functionality and Calibration-Free Measurements. *Sens. Actuators B Chem.* **2025**, *443*, 138231. [CrossRef]
214. Kazanskiy, N.L.; Golovastikov, N.V.; Khonina, S.N. The Optic Brain: Foundations, Frontiers, and the Future of Photonic Artificial Intelligence. *Mater. Today Phys.* **2025**, *58*, 101856. [CrossRef]
215. Xu, X.; Ren, G.; Feleppa, T.; Liu, X.; Boes, A.; Mitchell, A.; Lowery, A.J. Self-Calibrating Programmable Photonic Integrated Circuits. *Nat. Photonics* **2022**, *16*, 595–602. [CrossRef]
216. Padmaraju, K.; Logan, D.F.; Zhu, X.; Ackert, J.J.; Knights, A.P.; Bergman, K. Integrated Thermal Stabilization of a Microring Modulator. *Opt. Express* **2013**, *21*, 14342–14350. [CrossRef]
217. Bonyár, A.; Kovács, R. Towards Digital Twins of Plasmonic Sensors: Constructing the Complex Numerical Model of a Plasmonic Sensor Based on Hexagonally Arranged Gold Nanoparticles. *Nanomaterials* **2023**, *13*, 2044. [CrossRef] [PubMed]
218. Maiberg, M. Toward Digital Twins by One-Dimensional Simulation of Thin-Film Solar Cells: Cu (In, Ga) Se_2 as an Example. *Phys. Rev. Appl.* **2024**, *21*, 034051. [CrossRef]
219. Xue, C.; Sun, H.; Tang, Y.; Wei, J.; Guo, J. Self-Powered Photonic Sensor Using Cholesteric Liquid Crystal Elastomer-Based Sandwiched Architecture with Mechanochromism and Triboelectric Response. *ACS Appl. Mater. Interfaces* **2025**, *17*, 46226–46237. [CrossRef]
220. Hu, Y.; Liang, B.; Fang, L.; Ma, G.; Yang, G.; Zhu, Q.; Chen, S.; Ye, X. Antifouling Zwitterionic Coating via Electrochemically Mediated Atom Transfer Radical Polymerization on Enzyme-Based Glucose Sensors for Long-Time Stability in 37 °C Serum. *Langmuir* **2016**, *32*, 11763–11770. [CrossRef] [PubMed]
221. Flexible Piezoelectric Materials and Strain Sensors for Wearable Electronics and Artificial Intelligence Applications. *Chem. Sci.* **2024**, *15*, 16436–16466. [CrossRef]

Disclaimer/Publisher's Note: The statements, opinions and data contained in all publications are solely those of the individual author(s) and contributor(s) and not of MDPI and/or the editor(s). MDPI and/or the editor(s) disclaim responsibility for any injury to people or property resulting from any ideas, methods, instructions or products referred to in the content.